공학석사 학위논문

Seismic Integrity Characteristics of Uncracked and Through Wall Circumferential Cracked Pipes under Beyond Design Basis Earthquake

설계기준 초과지진에 대한 비균열 및
원주방향 관통균열 배관의 내진 건전성 특성

2014 년 2 월

서울대학교 대학원

에너지시스템공학부 원자핵공학 전공

김 예 지

Seismic Integrity Characteristics of Uncracked and Through Wall Circumferential Cracked Pipes under Beyond Design Basis Earthquake

지도 교수 황 일 순

이 논문을 공학석사 학위논문으로 제출함
2013 년 12 월

서울대학교 대학원
에너지시스템공학부 원자핵공학전공
김 예 지

김예지의 공학석사 학위논문을 인준함
2013 년 12 월

위 원 장 Takuji Oda (인)

부위원장 황 일 순 (인)

위 원 오 영 진 (인)

Abstract

Seismic Integrity Characteristics of Uncracked and Through Wall Circumferential Cracked Pipes under Beyond Design Basis Earthquake

Yeji Kim

School of Energy System Engineering

The Graduate School

Seoul National University

With technological improvements in design and construction, the magnitude of safety shutdown earthquake (SSE) is increasing for several new nuclear power plants (NPPs). However, in recent years we have witnessed a few prominent examples of beyond design basis events near nuclear power plants (NPPs), including the Fukushima in Japan and the North Anna in U.S.A.. As a follow-up to the Fukushima accident, old NPPs in EU and Korea are being subjected to stress tests to evaluate the integrity of their safety shutdown function under extreme conditions. In this procedure, the potential magnitude of an earthquake is reevaluated through a probabilistic approach. In light of these, it is becoming difficult to ignore the probability of earthquake exceeding the design basis.

Furthermore with the expected evolution of cracks in pipes of NPPs, it has become very important to monitor the integrity of the plant structure. In particular, in weldments of piping in the pressurized water reactor (PWR)

primary system, such as pressurizer surge line nozzles, cracks are likely to initiate and grow with time owing to various environmental effects. Presently, certain non-destructive examination methods are applied for detecting such cracks in pipes; however, these can only be applied at 10 years of the inspection period. In addition, to avoid the unnecessary replacement of components, the American Society of Mechanical Engineers Boiler and Pressure Vessel (ASME B&PV) Code Sec. XI specifies an allowable flaw size. Although we noted that some unexpected cracks were detected. Therefore, from a long-term viewpoint, it is essential to consider cracks in pipe analysis.

Toward this end, the present thesis focuses on seismic analysis for uncracked and cracked pipes to understand the dynamic behavior of the structure under a beyond design basis earthquake.

According to the ASME B&PV Code Sec. III, a pipe under seismic loading is subjected to two types of loads: the seismic inertial moment (M_{SI}) due to vibration and the seismic anchor motion moment (M_{SAM}) due to relative displacement between multiple anchors. The response spectrum analysis can be used to calculate M_{SI}, and seismic anchor motion analysis can be used to calculate M_{SAM}. These analyses are general procedures, but they can be used to provide the values of these two loads separately. In contrast, a time history analysis can be used to consider two loads simultaneously and provide a more realistic solution. This study aimed to (i) understand the characteristics of each method and then (ii) compare the dynamic behavior of uncracked and cracked pipes using time history analysis using ABAQUS that is a commercial finite element analysis tool.

First, an uncracked pipe was analyzed using general seismic analysis and time history analysis to understand the characteristics of each method. It was found that time history analysis generally produced a less conservative solution.

Then, various conditions were considered in cracked pipe analysis—pipe length, crack position, and excitation mode. The crack was simulated using "hinge element" which is one of connector element in ABAQUS. It was confirmed that the applied load on the pipe can decrease by 4-70% owing to cracks; however, it is difficult to find a clear trend that can explain all cases.

Additional computations were performed using a simplified model and conditions, and a qualitative interpretation of the complicated cracked pipe analysis result was performed. The main factors that can affect the change in the safety margin under seismic load are (i) the magnitude of the effect of a crack evolution on the change in stiffness and (ii) the relation between the natural frequency of the structure and the applied vibration.

Since the Fukushima accidents the evaluation of the structural integrity of NPP pipings is moving from a deterministic approach to a probabilistic analysis. To calculate the probability of pipe rupture, the exact prediction of the dynamic behavior of a pipe under particular conditions may be a key point. Therefore, the ultimate application of this thesis results is defined to provide complete measures for probabilistic fracture mechanics.

Key words : Seismic analysis of pipe, Beyond design basis earthquake, Time history analysis, Circumferential through-wall cracked pipe, Seismic inertial moment, Moment due to seismic anchor motion
Student number : 2012-20994

Contents

List of Tables

List of Figures

Chapter 1 Introduction

1.1 Beyond design basis earthquake, and the follow-up

Recent years have witnessed a few prominent examples of beyond-design-basis events near nuclear power plants (NPPs). Of these, the Fukushima accident in March 2011 is, of course, the most well-known. Previously, in July 2007, Tepco's Kashiwazaki Kariwa NPP was struck by the Niigata Chuetsu-Oki earthquake, which had a peak ground acceleration of 0.68g. More recently, in August 2011, the North Anna NPP was struck by an earthquake with a peak ground acceleration of 0.255g, which was much higher than its design basis of 0.18g. Earthquakes accompanied by tsunamis exceeding the design criteria have struck NPPs both with and without adverse effects(Ian).

After March 2011, efforts began in Europe to prevent unexpected damage to an NPP. As a follow-up to the Fukushima accident, old NPPs were subjected to stress tests to evaluate the integrity of their safety shutdown function under extreme conditions. These stress tests involved four steps: (i) seismic hazard analysis, (ii) accident sequence analysis, (iii) seismic fragility evaluation, and (iv) seismic margin evaluation(F. Godefroy, 2012).

In this procedure, the potential magnitude of an earthquake is considered through a probabilistic approach(KINS, 2013; Reed et al., 1991). For example, for the Wolsung 1 plant in Korea, a 0.3g earthquake having a

probability less than 10^{-4} per year was considered in the stress test, whereas the design basis earthquake is 0.2g (Korea Hydro & Nuclear Power Company, 2013). Then, after assuming a hypothetical accident scenario that can affect the core integrity, a seismic fragility assessment is performed for the components under this scenario(U.S. Nuclear Regulatory Commision, 2009, 2012a). In light of the risks of ignoring the probability of earthquakes exceeding the design basis, I believe that it is also essential to evaluate the safety margin of pipes in the event of a beyond design basis earthquake.

1.2 Nondestructive evaluation of cracks in pipes in old NPPs

With the expected extension of the life of NPPs, it has become very important to monitor the integrity of the plant structure. In particular, in the weldment of piping in the primary system, such as surge line nozzles, cracks are likely to occur owing to various environmental effects. Presently, some non-destructive examination methods are available for detecting such cracks; however, these can only be applied after 10 years of the inspection period(Yoon et al., 2013). Furthermore, to avoid the unnecessary replacement of components, the American Society of Mechanical Engineers Boiler and Pressure Vessel (ASME B&PV) Code sec. XI specifies an allowable flaw size (ASME). If the detected crack size is smaller than the allowable size, plant operation can continue until the next inspection period.

However, this approach has some drawbacks. First, some unexpected cracks were detected. The probability of detecting cracks whose depth is

less than 20% of the pipe thickness is very high(Selby & Harrington, 2009). Furthermore, the crack growth rate is considered and duly weighed when calculating the allowable flaw size. However, we have noted the detection of cracks that far exceed the allowable criteria, including through-wall thickness cracks(Gorman, Hunt, Riccardella, & White, 2009). In addition, the allowable flaw size according to the ASME B&PV Code sec. XI is calculated from the load applied on the uncracked pipe, and this may produce an excessively conservative result. Therefore, dynamic behavior analysis of a cracked pipe is urgently required.

1.3 Objective

With improvements in design and construction technologies, the magnitude of safety shutdown earthquake(SSE) is increasing in several new NPPs. In addition, the operational life of NPPs are being extended beyond 60 years in countries with mature nuclear technology. As mentioned above, it is imperative that the probability of beyond design basis earthquakes not be neglected anymore.

Toward this end, the present study focuses on seismic analysis for uncracked and cracked pipes to understand the dynamic behavior of the NPP structure under beyond design basis earthquakes.

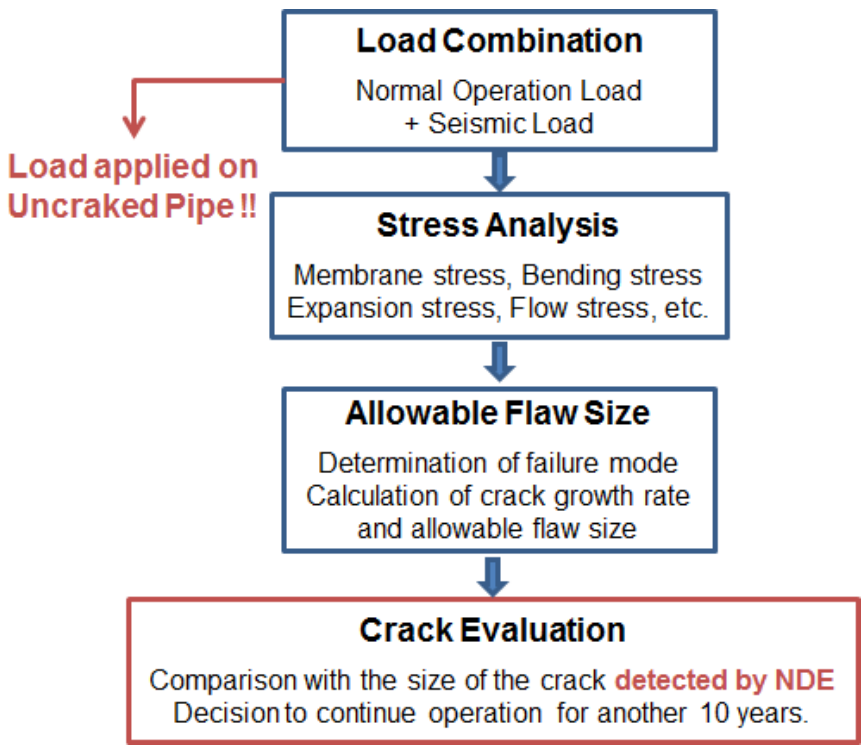

Figure 1.1 Process for calculating allowable crack size(ASME)

Chapter 2 Literature Review

This section presents a review of references and related materials as a step toward defining the main problem. First, several criteria and standards regarding seismic effects on the structure of an NPP are examined. Then based on the outcomes and limitations of previous studies, the problem definitions and research design are determined.

2.1 Seismic loading

2.1.1 Loading type

A pipe under seismic loading is subjected to two types of loads: the seismic inertial moment (M_{SI}) due to vibration and the seismic anchor motion moment (M_{SAM}) due to relative displacement between multiple anchors. The maximum values of the two loads calculated from finite element analysis are used in the stress analysis and then reflected in the seismic design of the structure if the stress does not exceed the allowable criteria.

The moment due to the earthquake is divided into two parts although both moments are applied simultaneously based on the ASME B&PV Code. According to sec. III of this code, an earthquake exceeding the safety

shutdown earthquake is classified as Level D operation condition, and the seismic moment can be divided into two types. Each type has criteria pertaining to the allowable stress limit, as given by the respective equations below.

$$B_1 \frac{PD_0}{2t} + B_2 \frac{D_0}{2I} M_I \leq 3.0 S_m$$

$$C_2 \frac{M_{SAM} D_0}{2I} \leq 6.0 S_m$$

where B_1 and B_2 denote the primary stress indices; P and I denote the design pressure and moment of inertia, respectively; D_0 and t denote the outside diameter and nominal wall thickness of the pipe, respectively; M_I denotes the seismic inertial moment; and M_{SAM} denotes the moment due to seismic anchor motion(ASME).

Because M_{SI} is only due to vibrations, if a perfectly uniform excitation is applied to the structure, it will experience only M_{SI}. However, in practice, a structure is subjected to nonuniform excitations, and therefore, M_{SI} and M_{SAM} are applied simultaneously.

2.1.2 Characteristics of major load

The ASME code sec. III specifies criteria to classify the stress in consideration of the failure mode. M_{SI} induces primary stresses that are produced by external loads such as pressure and dead weight. This type of stress can induce plastic collapse because once plastic deformation begins, it continues till the failure of the structure.

M_{SAM} can cause secondary stresses that are generally produced by thermal gradients or structural dislocation. The standards for secondary stress are generally less strict than those for primary stress because the secondary load tends to dissipate as the system deforms through yielding(ASME).

However, we have noted that because seismic loading is a repeated load, unexpected seismic anchor motions have a greater probability of causing pipe failure than the seismic inertial moment (Nam, Bae, Huh, & Kim, 2011), as though the secondary stresses can cause fatigue fractures. Therefore, for analyzing the pipe behavior, nonuniform excitation cases are very important.

2.2 Seismic analysis of pipes

2.2.1 General analysis procedure

Using a general analysis procedure, M_{SAM} and M_{SI} can be obtained separately as shown in Figure 2.1. There are two steps, the containment building has to be preceded before pipe analysis because movement at particular points of the building would represent the motion of the anchors that support the pipes.

The seismic response of the containment building can be obtained from time history analysis using the time history of the ground acceleration as the

input. The response output includes not only the acceleration response but also the velocity and displacement responses.

Using these results of the containment building analysis, the seismic analysis of the pipe can be conducted by various methods. First, the response spectrum converted from the time history of acceleration can be used for response spectrum analysis to calculate the inertial moment (M_{SI}). The moment due to the relative displacement between multiple anchors (M_{SAM}) can be determined using the displacement time history.

2.2.2 Time history analysis

In the seismic analysis, we can use the acceleration time history for an analysis called the time history analysis. This method can provide a more practical result because both moments are considered simultaneously. However, it is very time-consuming. In addition, the ASME B&PV code does not specify any criteria pertaining to the summation of two loads, and therefore, this method is not a general one.

2.3 Experimental analysis of dynamic behavior of pipe under seismic loading

Some previous studies have focused on the behavior of a pipe under seismic loading. In Japan, JNES used a 1/3 scale recirculation pipe and

applied uniform excitation using a single shaking table (Suzuki & Kawauchi, 2008; Suzuki, Kawauchi, & Abe, 2006). This test was one of the most advanced ones in that the pipe had cracks and simulated components were included. However, only the seismic inertial moment was considered in this test.

Recently, a pipe integrity experiment under nonuniform excitation was conducted at Pusan National University (Seo, 2013). In this experiment, two shaking tables were used; however, this experiment is limited to the case of an uncracked pipe, and analytical studies were not performed.

2.4 Computational analysis of dynamic behavior of pipe under seismic loading

The Engineering Mechanics Corporation of Columbus (EMC^2) analytically verified JNES's experiment. They simulated a crack using a connector element, which is a contact component in ABAQUS. They found that pipe failure can be well predicted when using a low cycle fatigue model. However, for the same reason, only the seismic inertial moment is considered(Zhang et al., 2010).

EMC^2 used the same analytical method to evaluate the margin of leak before break of main steam line of the Atucha II NPP. Their results showed that the critical crack size under a design basis earthquake is 94% of the circumference for a through-wall crack. When 33% of the circumference

cracks, pipe rupture occurs when the magnitude of the applied earthquake is 25g(Wilkowski et al., 2011; Zhang et al., 2012, 2013). Considering that the magnitudes of the design basis earthquakes of almost NPPs are 0.2–0.3g, the piping systems already have very high safety margin against earthquakes. However, this analysis was restricted to a few pipe geometries, and therefore, various other pipe geometries and load conditions should be considered.

In summary, a computational analysis of uncracked and cracked pipes in consideration of nonuniform excitation that can cover both seismic inertial and seismic anchor motion moments can be of great importance. The next chapter provides details about the problem definition and rationale of this study.

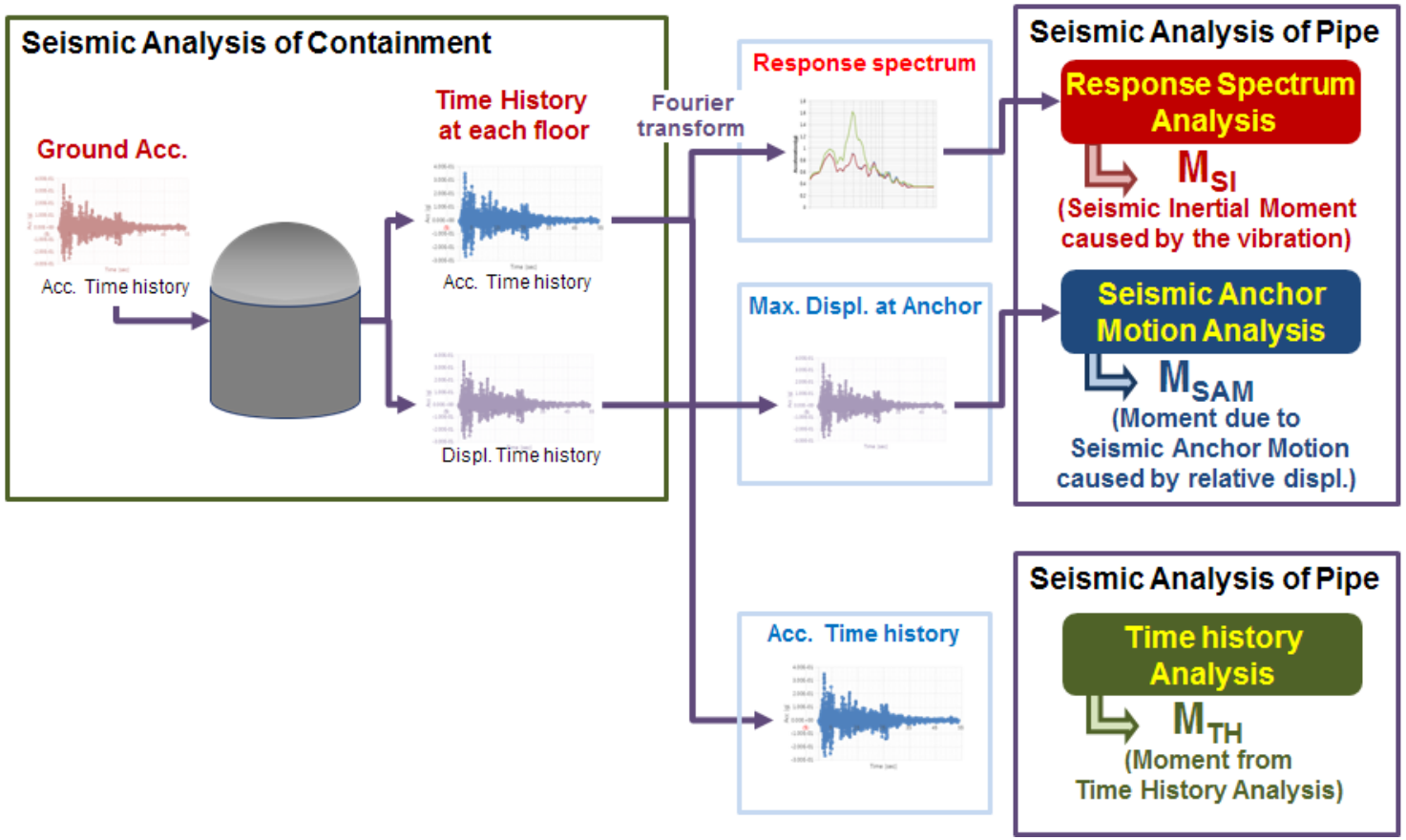

Figure 2.1 Scheme of seismic analysis of pipe

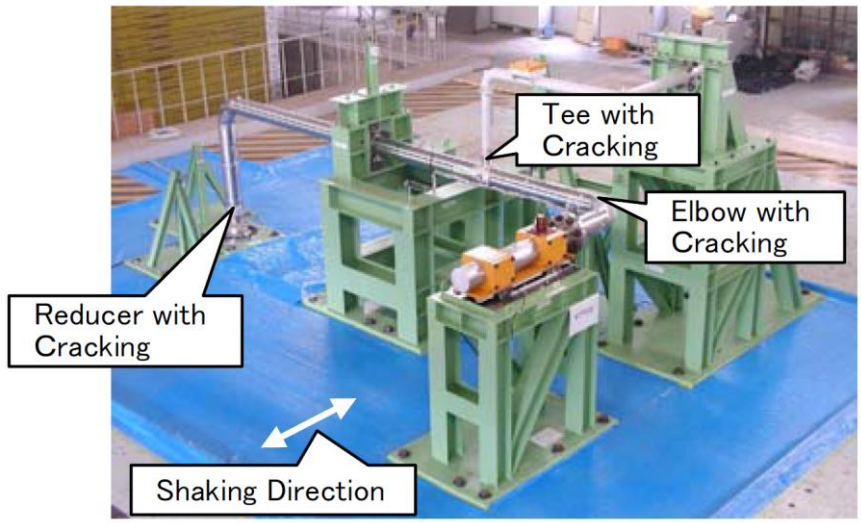

Figure 2.2 Photo showing JNES's test : Experiment on behavior of cracked pipe under uniform excitation(Suzuki & Kawauchi, 2008)

Figure 2.3 Photo showing Pusan National University's test : Experiment on behavior of uncracked pipe under nonuniform excitation(Seo, 2013)

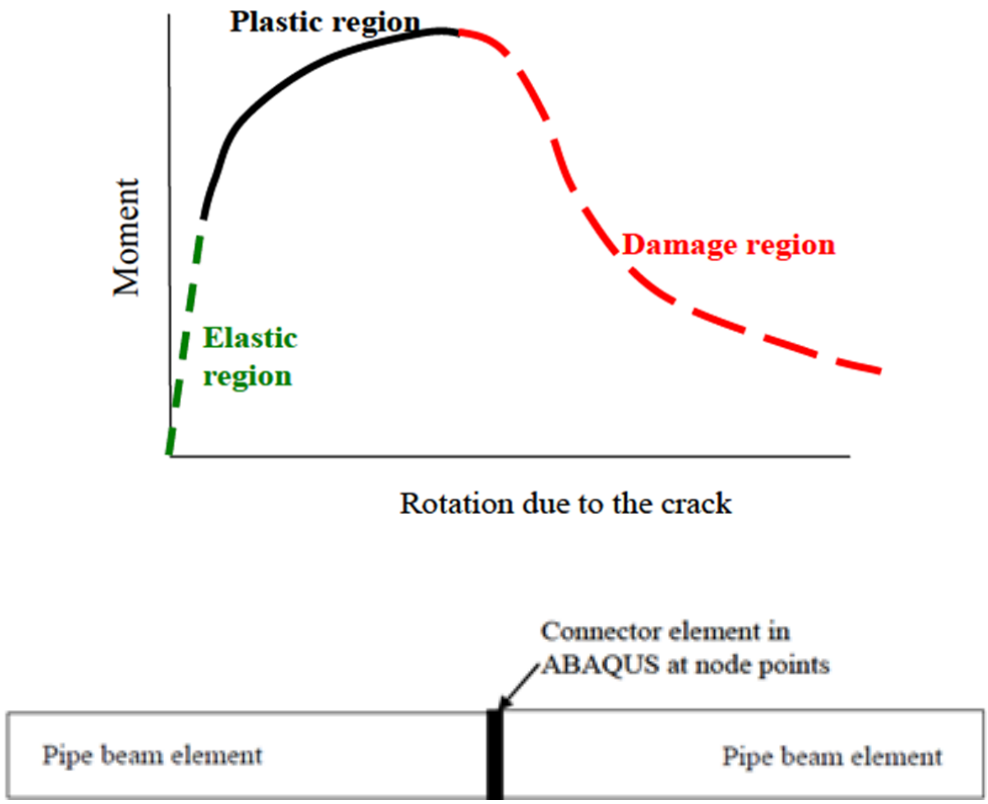

Figure 2.4 Simulation of a crack using connector element(Zhang et al., 2010)

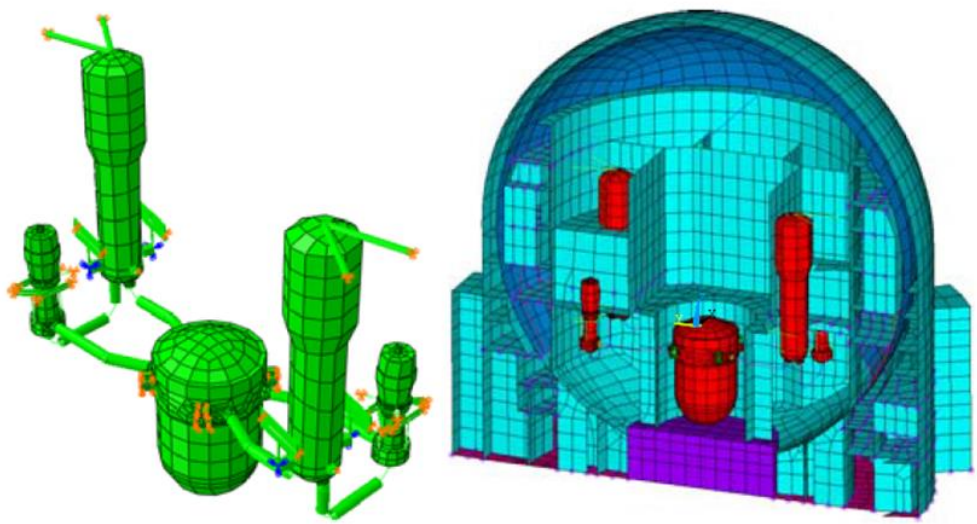

Figure 2.5 Modeling of Atucah II nuclear power plant for seismic analysis(Wilkowski et al., 2011)

Chapter 3 Research Design

3.1 Problem definition and goals

As mentioned above, recent events such as the Fukushima accident have led to an increased need for understanding the dynamic behavior of pipes under seismic loading. As a continuation of previous studies, the cracked pipe behavior under nonuniform excitation in consideration of the seismic anchor motion must be analyzed.

According to the ASME B&PV code, the load due to the earthquake applied to a structure can be classified into two types (M_{SI}, M_{SAM}), and each value can be calculated by general seismic analysis. However, this method only provides the maximum value of the moment under a particular condition, and it is not appropriate for understanding the dynamic behavior history of a structure. In contrast, time history analysis can provide a more realistic and full-time solution, and therefore, the first objective of this study is to understand the characteristics of time history analysis.

The second objective of this study is a comparison between the dynamic behavior of uncracked and cracked pipes using time history analysis. This analysis can provide an understanding of the effect of cracks on the behavior of a pipe under dynamic loading.

3.2 Seismic analysis scheme

A general seismic analysis procedure involves two main steps: containment building analysis and pipe analysis. The results of containment building analysis for each floor, which represent the motion of the anchors, can be used as the input for pipe analysis. Sections 3.3 and 3.4 describe the details of each analysis method.

To achieve the first objective mentioned above, response spectrum analysis, seismic anchor motion analysis, and time history analysis were conducted for an uncracked pipe. Only time history analysis was conducted for a cracked pipe, the results of which were compared with those for the uncracked pipe. All calculations were performed using ABAQUS v6.12.

3.3 Seismic analysis of containment building

3.3.1 Model

The analysis model was based on the geometry and material properties of OPR-1000. Although its building height is 66 m, a region from the base up to a height of 27.5 m, where all the piping systems are located, was focused upon. The building was fabricated from post-tensioned concrete, and the damping of the entire building was 5%.

The building contains primary and secondary walls and slabs where

components are linked or supported. However, it was simulated without these walls and slabs for simplifying the analysis. S4R, a shell element in ABAQUS, was applied. Figure 3.2 and Figure 3.3 show the geometry and mesh model of the building analysis.

3.3.2 Input data

In seismic design and structural analysis, the acceleration of an artificial earthquake is actually used. However, in this case, the acceleration history of the El Centro earthquake, which has vibrations of various frequencies, is used for the analysis("El Centro Earthquake Vibrationdata,"). All history data for three 3 orthogonal directions—one vertical and two horizontal—were used; the data points of each history have a spacing of 0.02 s.

According to the regulatory guide, the earthquake acceleration time history should be sufficiently long (U.S. Nuclear Regulatory Commision, 2007b, 2007c). The time history used in this study was 53.4 s long with a peak occurring at ~6 s, as shown in Figure 3.4.

3.3.3 Output : data generated for pipe analysis

Because the earthquake acceleration was applied to the base floor of the building, the higher the position, the greater is the response at each floor. For a conservative structural analysis, the response data of the bottom (0a) and the top (5a) of the pipe region was selected. Figure 3.5 to Figure 3.7

show example results of the containment building analysis. The data points of the output history have a spacing of 0.01 s.

Figure 3.5 shows the displacement at each position for seismic anchor motion analysis. As shown in Figure 3.6, the relative displacement between two positions is very small compared with each displacement, even though the distance between the two positions is 27.5 m. Figure 3.7 shows the acceleration time history, which can be used in time history analysis.

For the response spectrum analysis, the acceleration time history should be converted into the frequency domain, which is called the response spectrum. Some modifications are needed before structural analysis (U.S. Nuclear Regulatory Commision, 1978), namely, the broadening and widening of peaks. Originally, the raw spectrum has many peaks, as shown in Figure 3.8; however, to account for uncertainties in the structural frequencies and material properties, the peak value should be broadened by a particular frequency range. In this analysis, $\pm$ 10% of frequency was applied as the broadening range.

3.4 Seismic analysis of pipe

3.4.1 Response spectrum analysis

This method is used to calculate the seismic inertial moment (M_{SI}) in the ASME B&PV Code. The anchors at each end of the pipe were fixed, and the

response spectrum was applied. One response spectrum was used for the uniform excitation case, and an enveloped spectrum obtained by taking the maximum values from the two spectrums was used for the nonuniform case.

Hundred natural frequency values were extracted, and the modal responses were combined by the square root of the sum of squares (SRSS) method according to the regulatory guide 1.92(U.S. Nuclear Regulatory Commision, 2012b).

3.4.2 Anchor motion analysis

By applying different displacement time histories of the building to each anchor, static analysis was conducted to calculate the moment due to seismic anchor motion (M_{SAM}). The duration of the time history was 30 s and the spacing was 0.01 s, and the maximum applied moment was chosen as M_{SAM}.

3.4.3 Time history analysis

A 30-s-long acceleration time history of the building was applied to the anchors of the pipe. One and two acceleration time histories were applied to each anchor for the uniform and nonuniform excitation case, respectively. To avoid the nonconvergence of the solution owing to the initial value of the acceleration, the initial velocity was set up.

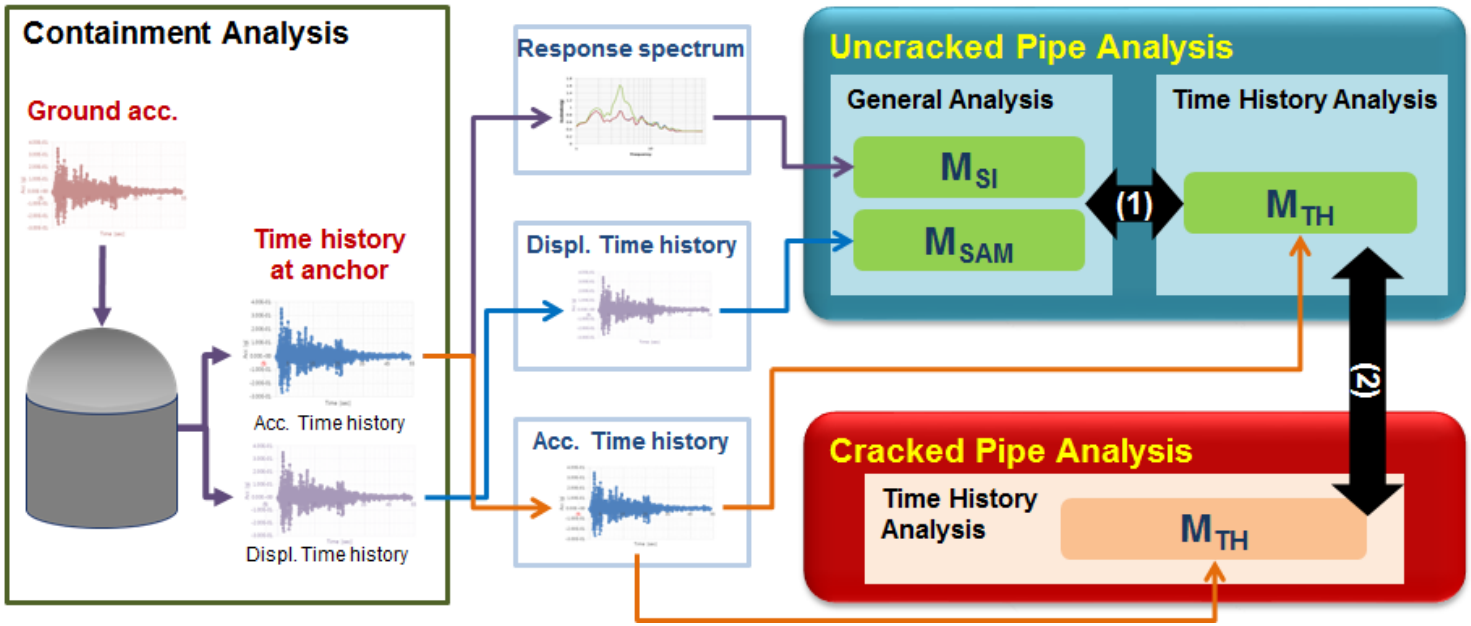

Figure 3.1 Analysis scheme of this study

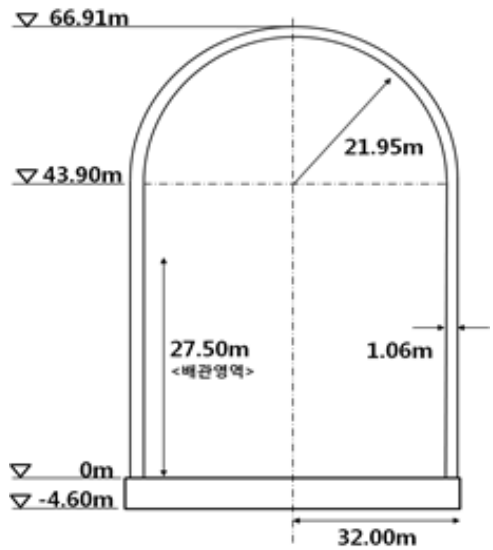

Figure 3.2 Geometry of containment building (referenced from OPR-1000)

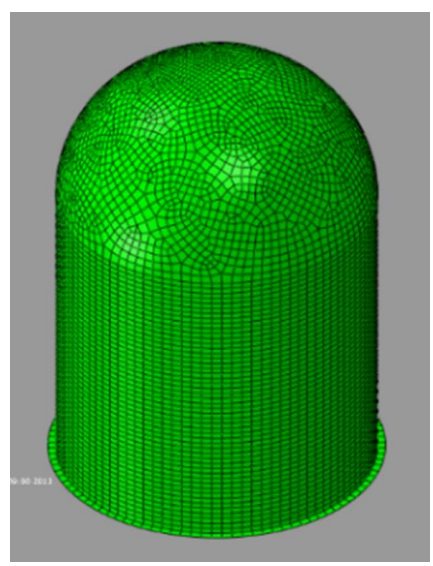

Figure 3.3 The modeling of containment building

Table 3.1 Properties of containment building

Material	Post-tentioned concrete
Density	2.4 g/mm^3
Young’s Modulus (E)	30400.8 MPa
Poisson's ratio	0.17
Damping ratio	5%

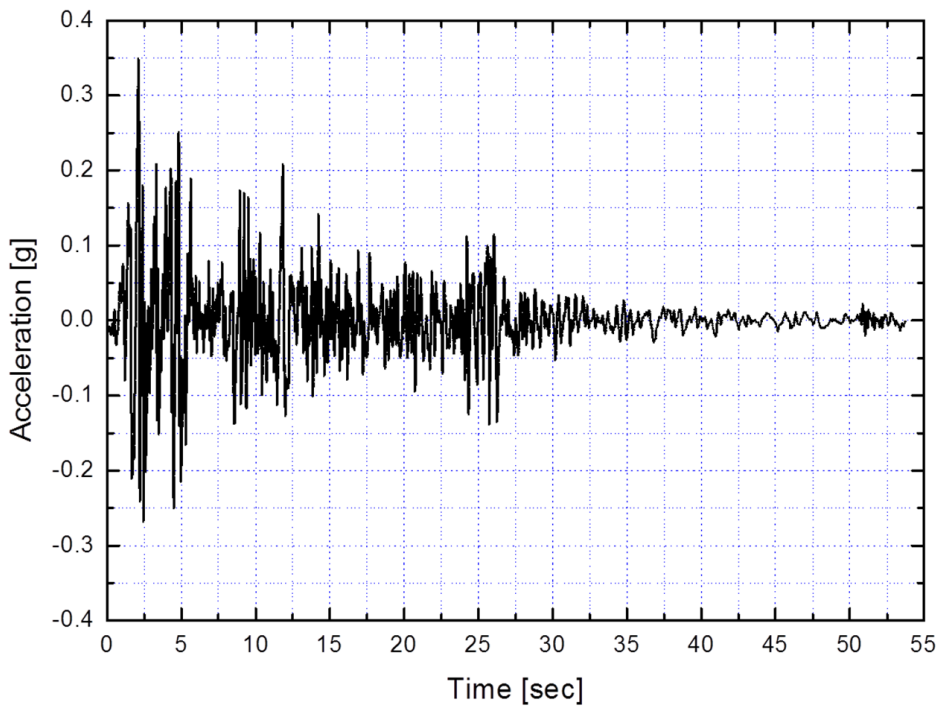

Figure 3.4 Time history of ground acceleration of El Centro earthquake (N-S direction)

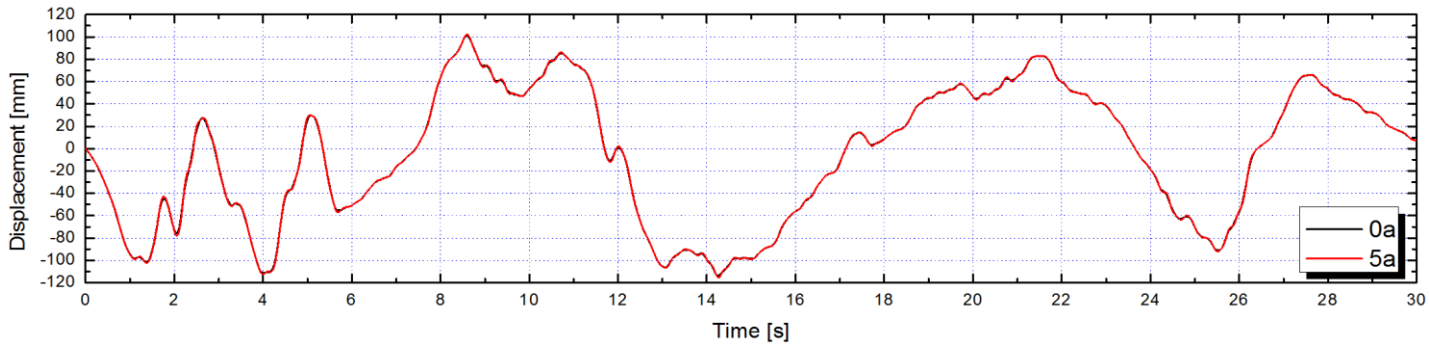

Figure 3.5 Result of containment building analysis: Displacement time history

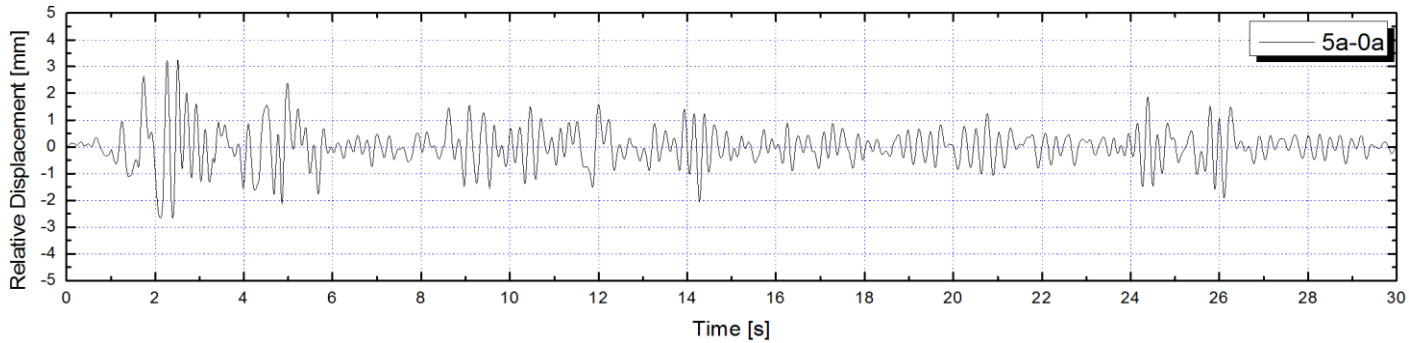

Figure 3.6 Result of containment building analysis: Relative displacement time history between 0a and 5a

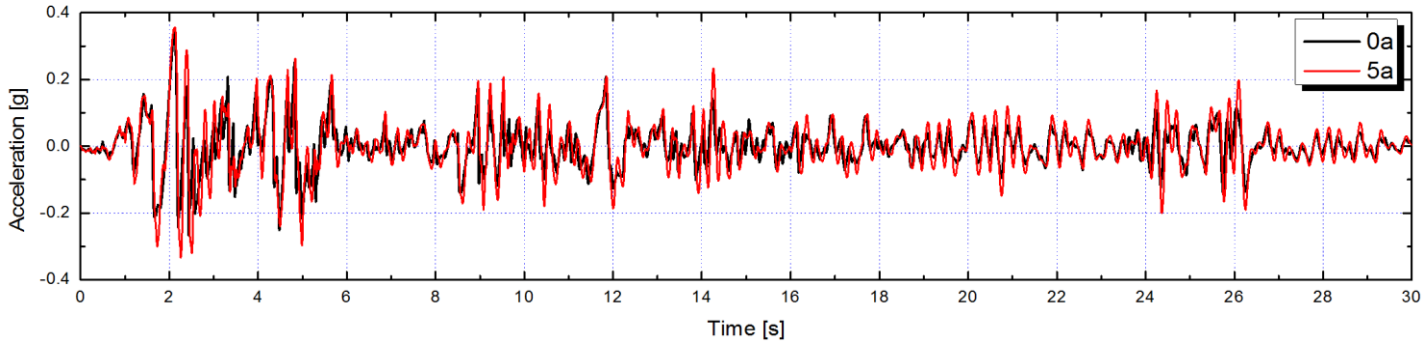

Figure 3.7 Result of containment building analysis : Acceleration time history

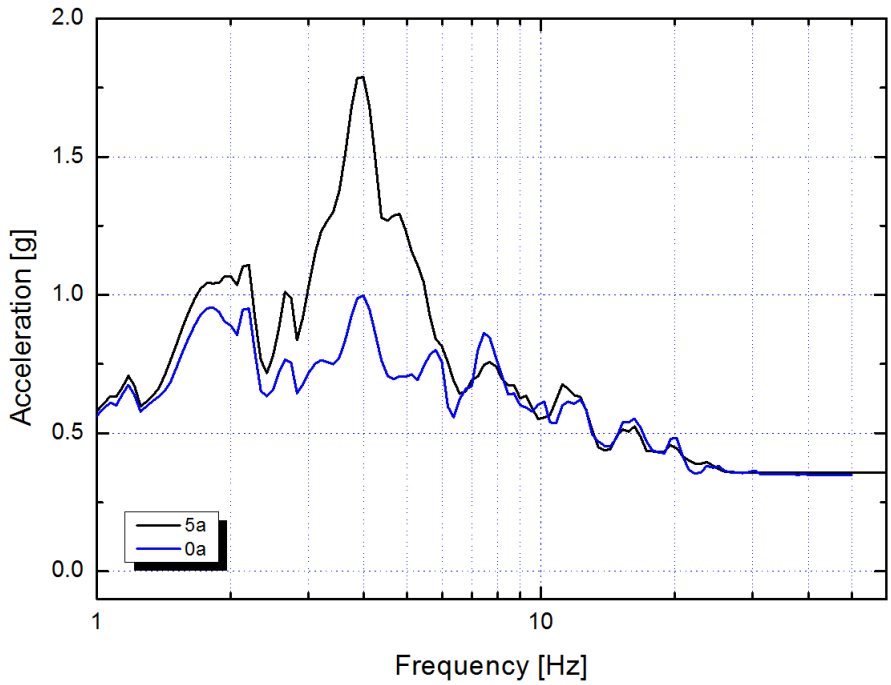

Figure 3.8 Result of containment building analysis

: Raw response spectrum

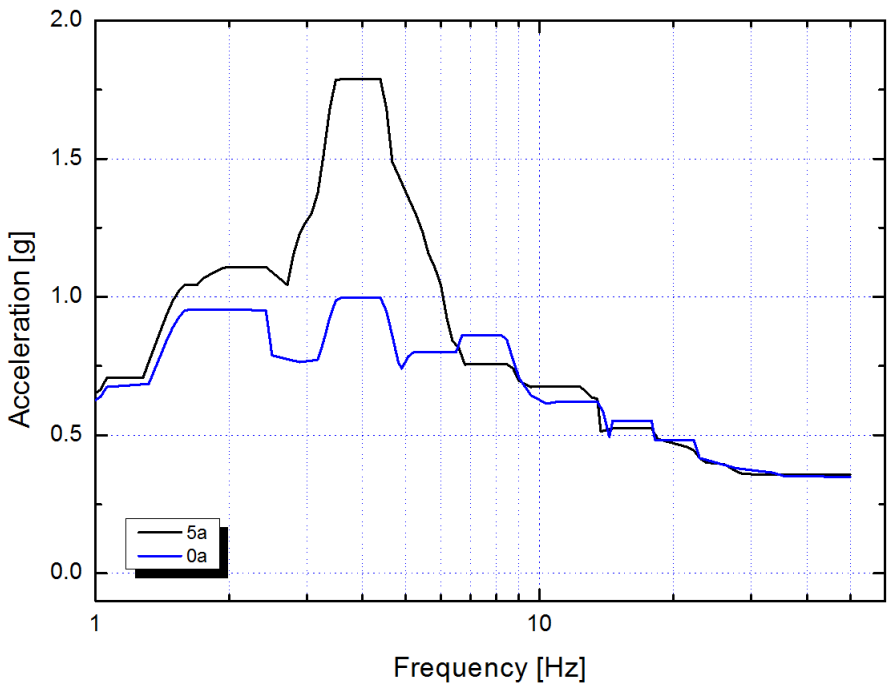

Figure 3.9 Result of containment building analysis

: Modified response spectrum

Chapter 4 Seismic Behavior of Uncracked Pipe

4.1 Purpose of analysis

First, the uncracked pipe was analyzed based on the result of the containment building analysis described in chapter 3. As mentioned above, two types of load (M_{SI} and M_{SAM}) are applied to the structure in the event of an earthquake, and the ratio of the two moments can vary depending on the geometry of the pipe. One of the representative variables of the geometry of the pipe is its length. Thus, the first purpose of the uncracked pipe analysis is to compare the contribution of the M_{SI} and M_{SAM} depending on the pipe length using the response spectrum analysis and seismic anchor motion analysis.

In addition, a comparison of the general analysis procedure that provides the values of M_{SI} and M_{SAM} separately and the result of the time history analysis that can consider two loads simultaneously was used to understand the characteristics of the each analysis. This is used in the next chapter to compare with the cracked pipe analysis.

4.2 Input and setup

4.2.1 Geometry and element

A simple straight pipe was assumed to understand the circumstances clearly. Four pipe lengths were considered—5, 10, 15, and 20 m—to determine the effect of pipe length and geometry. The pipe was simulated by using a two-node beam element in ABAQUS.

4.2.2 Material

The pipe model used was 12-inch schedule 160 and fabricated from TP 316 Stainless steel, which is the most common type used for the branch line in the primary system.

To account for the water inside the pipe, the revised density was used. When we assume the mass of the pipe that has 323.8-mm diameter and 33.3-mm thickness with the water, the density is 9.71 g/cm^3.

4.2.3 Damping

The damping ratio was 4%, and the damping coefficient followed the Rayleigh damping model as explained in regulatory guide 1.61(U.S. Nuclear Regulatory Commision, 2007a).

4.2.4 Setup

The nonuniform excitation case should be considered to account for the condition in which both M_{SI} and M_{SAM} are applied to the structure

simultaneously. In the response spectrum analysis, the enveloped response spectrum was used, and the two anchors were fixed. For the seismic anchor motion analysis and time history analysis, the two displacement and acceleration time histories were applied to each anchor, and five degrees of freedom (except the vibration direction) of the anchors were constrained.

4.3 Contribution of M_{SI} and M_{SAM}

Figure 4.2 and Figure 4.3 show the contributions between M_{SI} and M_{SAM} for each pipe length. The X-axis represents the normalized distance from anchor 1 and the Y-axis, the normalized moment. Each moment was normalized by the maximum value of (M_{SI} + M_{SAM}) for each pipe length.

For the inertial moment, the curve has a W shape with the maximum values at both anchors. When we consider that this data is the absolute value, it is observed that the shape of the curve is similar to the shape of the first mode vibration. As shown in Figure 4.3, M_{SAM} is lowest at the center of the pipe.

The seismic inertial moment is induced by vibrations, and therefore, it can be linked closely with the natural frequency of the structure or the stiffness. Table 4.2 shows that as the pipe length increases, the natural frequency of the pipe decreases, and this means that the long straight pipe can vibrate easily. The response spectrum analysis result shows good agreement with this statement. On the other hand, a pipe that has greater

stiffness can be affected by the difference between the displacement of the two anchors, and therefore, the contribution of M_{SI} of the 5-m pipe is the largest.

4.4 Characteristics of general analysis and time history analysis

The result of the time history analysis is indicated in Figure 4.4 to Figure 4.7 by a blue line. The black lines in each graph represent the M_{SI} (W shape) and M_{SAM} (V shape). For a 15- and 20-m pipe whose inertial moment is dominant, the curve of the time history result resembles the response spectrum analysis result. When the MSAM is dominant (5-m pipe), the time history analysis curve is similar to the seismic anchor motion analysis result.

For the sake of comparison, the summation of M_{SI} and M_{SAM} is plotted as a red dash line, although there are no criteria pertaining to the summation of two moments in the ASME B&PV code. The value of the time history analysis is always less than that of the summation, indicating that the general analysis method is more conservative. However, as in the 5-m case, conservatism could decrease when the moment due to the seismic anchor motion is very dominant.

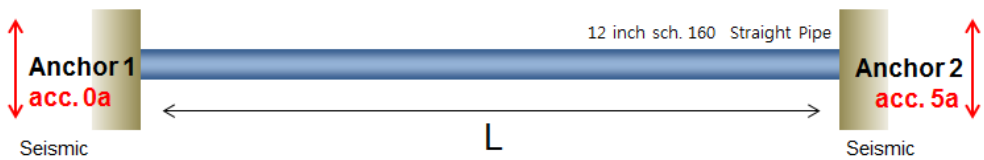

Figure 4.1 Modeling of uncracked pipe

Table 4.1 Properties of uncracked pipe

Pipe length	5m, 10m, 15m, 20m
Outer diameter	323.8 mm
Nominal thickness	33.3 mm
Number of nodes	100
Density	9.71 g/cm^3
Damping ratio	4%

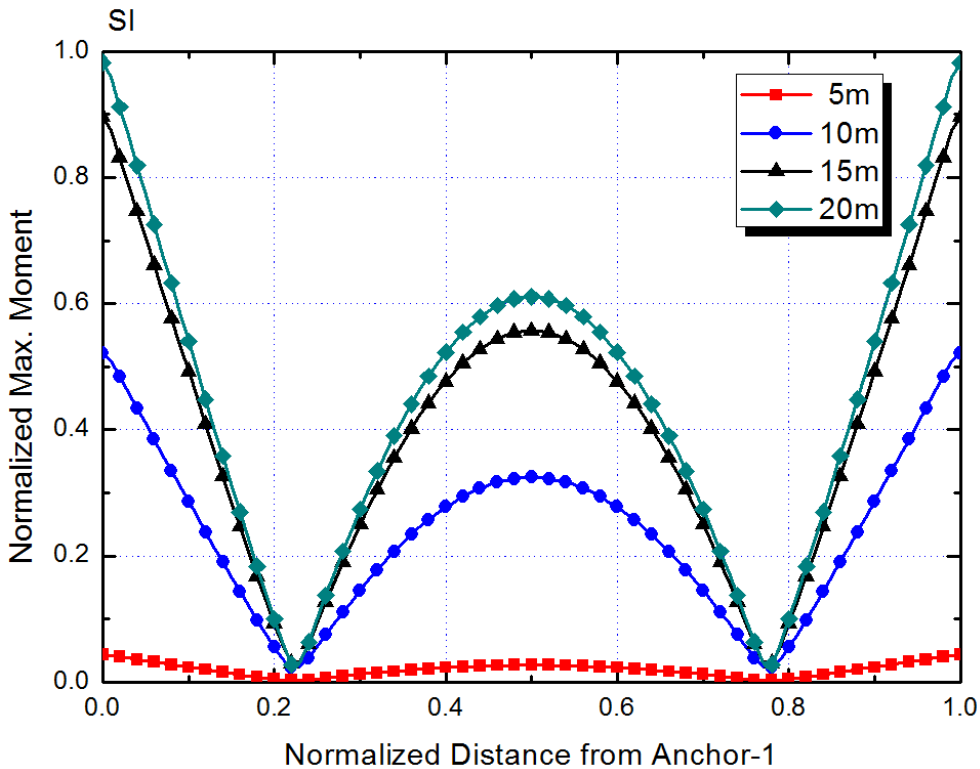

Figure 4.2 Normalized seismic inertial moment

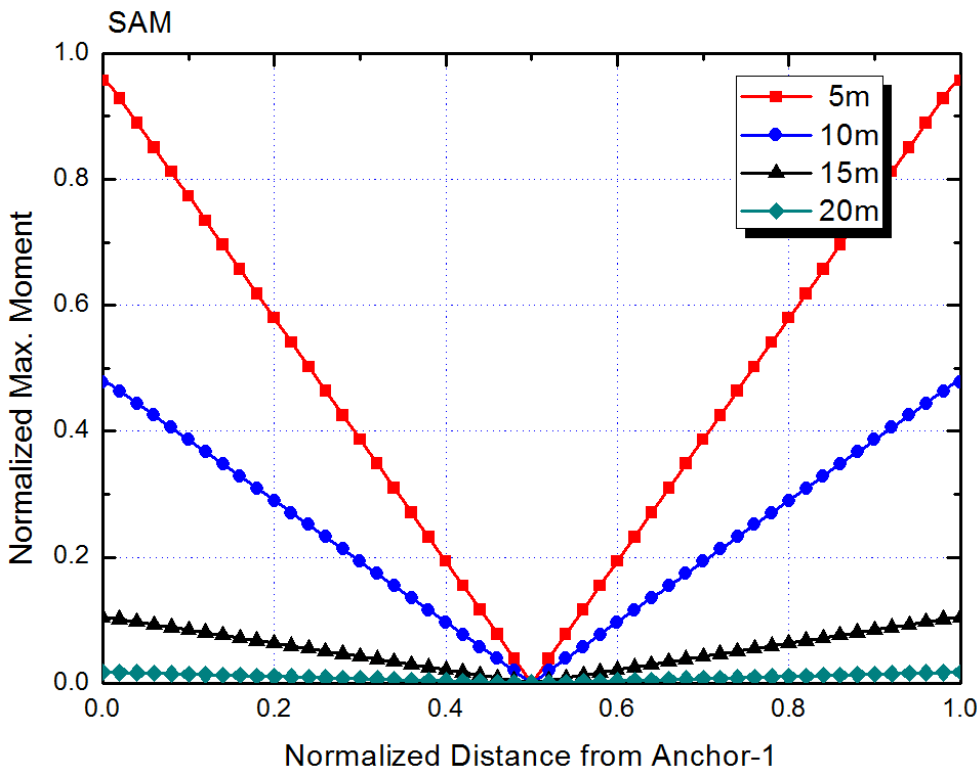

Figure 4.3 Normalized moment due to seismic anchor motion

Table 4.2 Natural frequency of uncracked pipe

MODE No.	Natural Frequency			
	5 m	10 m	15 m	20 m
1	58.91	15.282	6.8407	3.8577
2	153.41	41.451	18.718	10.589
3	281.62	79.601	36.342	20.644
4	423.31	128.36	59.361	33.889
5	433.56	186.4	87.437	50.206
6	602.19	211.65	120.19	69.458
7	782.39	252.41	141.1	91.489
8	846.51	325.14	157.23	105.83
9	970.58	403.48	198.14	116.14
10	1164.2	423.26	242.52	143.23
11	1269.5	486.44	282.17	172.6
12	1361.5	573.19	290.01	204.06
13	1561	634.75	340.23	211.63
14	1692.2	663	392.86	237.45
15	1761.8	755.28	423.17	272.61
16	1963.1	846.09	447.59	309.36
17	2114.4	849.52	504.13	317.38
18	2164.4	945.3	562.24	347.57
19	2365.2	1042.2	564.06	387.08
20	2536.2	1057.2	621.69	423.05
21	2565.2	1140	682.26	427.76
22	2764	1238.5	704.82	469.47
23	2957.3	1268.1	743.78	512.11
24	2961.1	1337.3	806.08	528.61
25	3024.3	1436.2	845.4	555.56

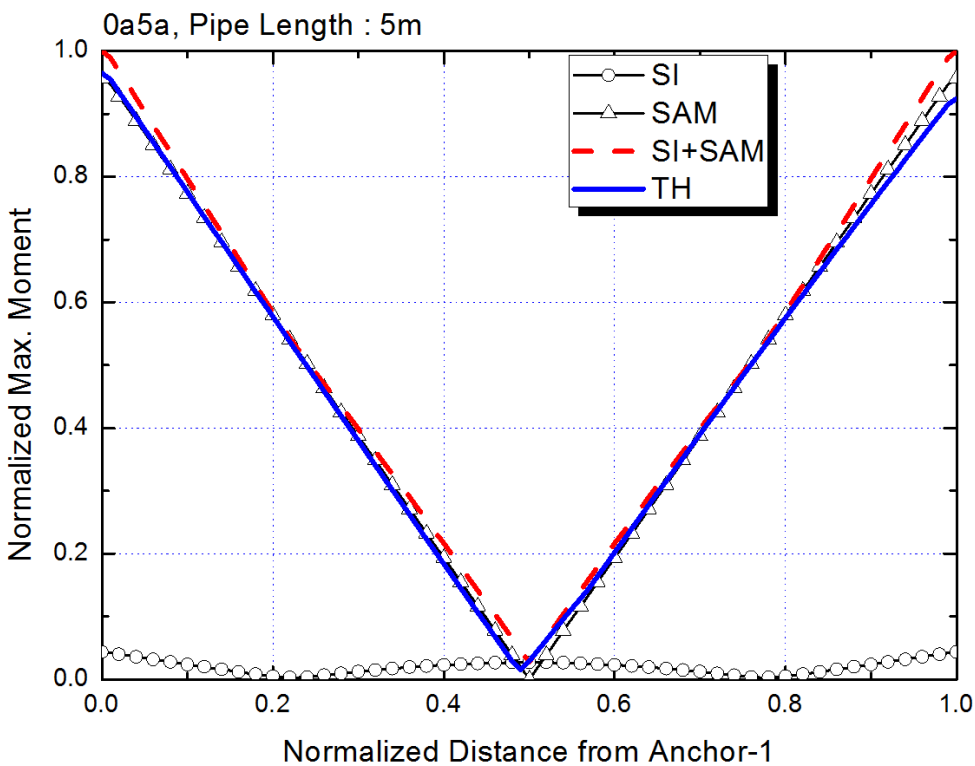

Figure 4.4 Comparison of time history result with general analysis procedure – 5-m pipe

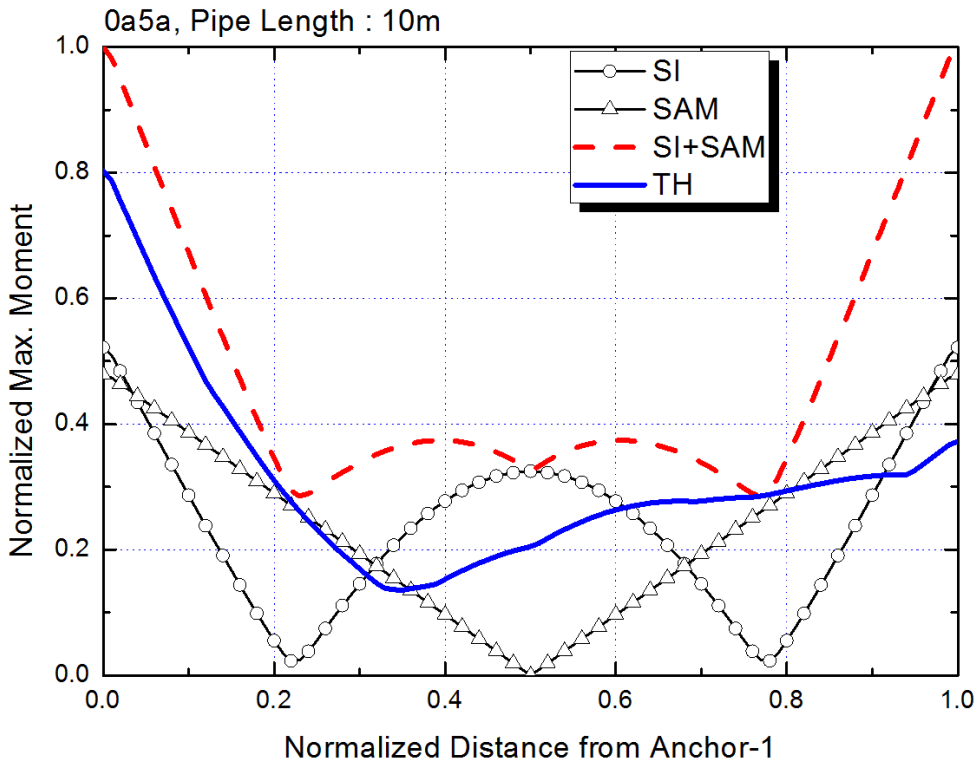

Figure 4.5 Comparison of time history result with general analysis procedure – 10-m pipe

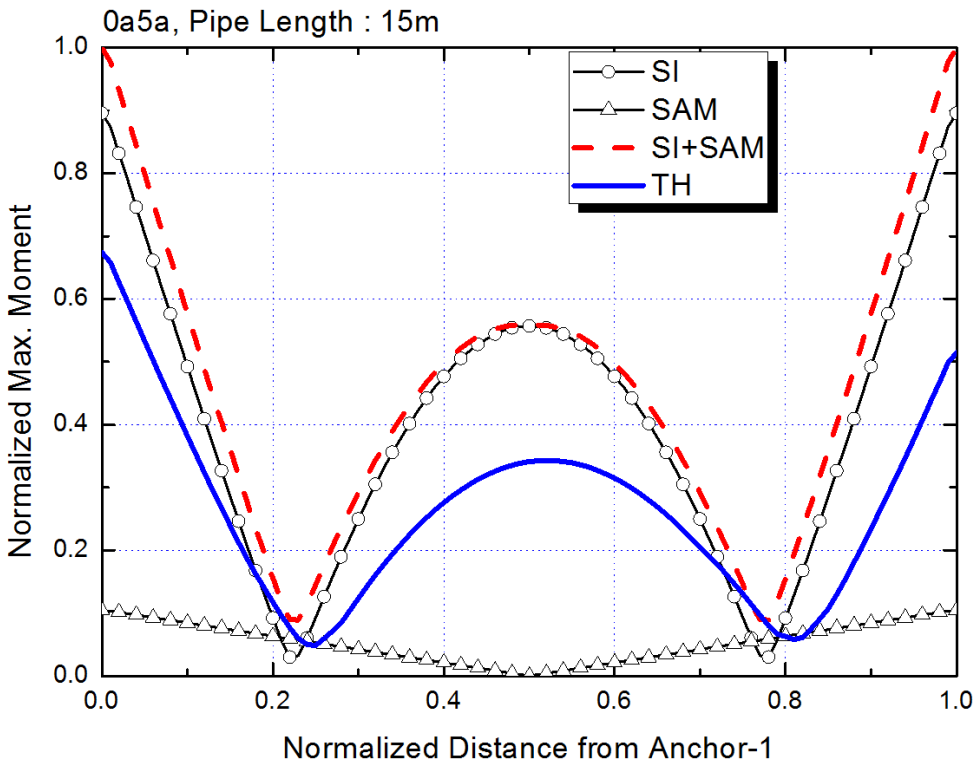

Figure 4.6 Comparison of time history result with general analysis procedure – 15-m pipe

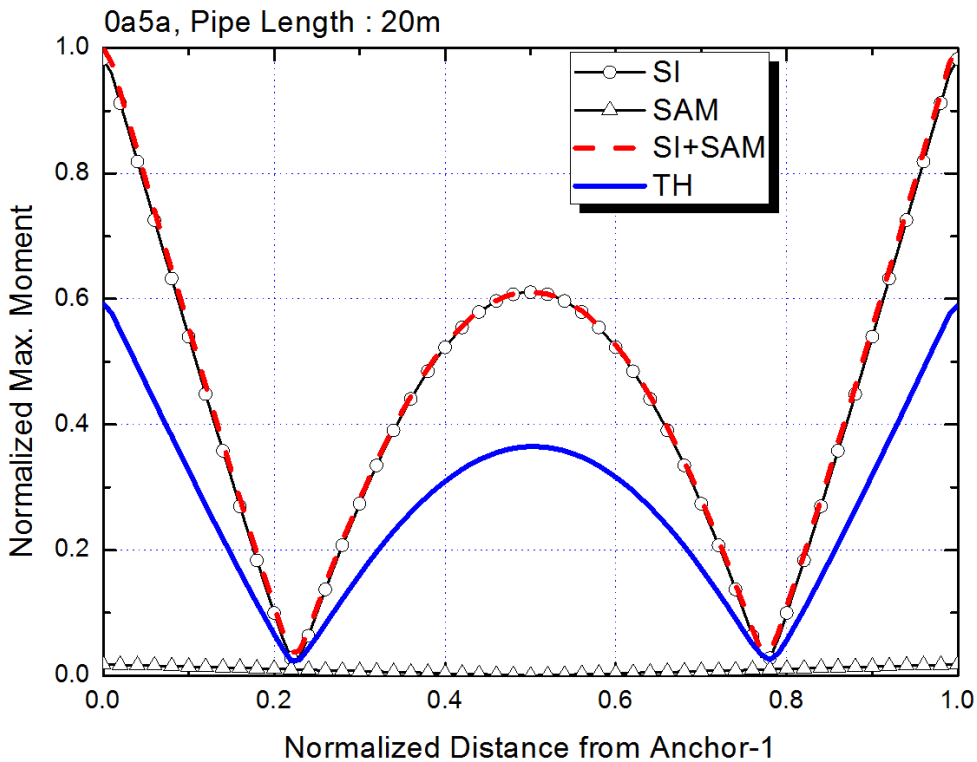

Figure 4.7 Comparison of time history result with general analysis procedure – 20-m pipe

Chapter 5 Seismic Behavior of Cracked Pipe

5.1 Purpose of analysis

In the previous chapter, the characteristics of the time history analysis were compared with the general analysis procedure. Using this time history analysis method, the calculation of both uncracked and cracked pipes was performed and compared. This chapter aims to understand the dynamic behavior of the cracked pipe under seismic loading. Then, the effect of the crack on the pipe behavior depending on the different conditions can be observed.

5.2 Input and setup

5.2.1 Geometry and element

The geometry and element used to describe the pipe region except for the crack was the same as that for the uncracked pipe. A hinge, which is one of the three node connectors in ABAQUS, was applied for simulating the crack based on the study conducted by EMC^2. The crack length was 1 mm, and a 50% circumferential through-wall crack was assumed.

The first node (Position A) where the applied moment is largest and the center of the pipe (Position B) where the applied moment is low were selected as the crack position to understand the position of the crack effect on the pipe behavior.

5.2.2 Material

The material was also the same as in the uncracked pipe case, TP 316 stainless steel. In addition, the mass of the connector is needed to avoid the mass matrix error. The connector mass was 295g because the crack length was 1 mm.

5.2.3 Damping

The damping ratio was 4%, and the damping coefficient followed the Rayleigh damping model as in the uncracked pipe case.

5.2.4 Setup

One (uniform excitation) or two (nonuniform excitation) acceleration time histories were applied to the anchors, but these were multiplied by the scale factor to control the loading applied at the crack. Because the uncracked pipe analysis was linear, the scale factor was derived by the ratio of the expected moment to the applied moment at the crack position on the

uncracked pipe. The scale factors used are listed in Table 5.2 and Table 5.3.

5.3 Description of cracked pipe behavior

5.3.1 Connector element

Connector elements are used for modeling physical connections. A hinge, one of the connector elements in ABAQUS, provides a revolute connection between two nodes(SIMULIA).

5.3.2 Behavior of connector element

The original use of the connector element is to simulate connect structures such as the hinge of a door, joint, etc. Therefore, some assumptions and techniques are required to make the connector element behavior similar to that for the cracked pipe.

First, one connector element was placed so that the pipe could be bent toward the crack open direction. However, if the pipe bends toward the crack close direction, it is difficult for the solution to converge owing to the contact problem. Therefore, one more connector element was used to limit the crack close. The arrangement of the two elements is shown in Figure 5.3.

Then, to make the compliance of connector element match with the cracked pipe, fracture mechanics analysis using a 3D solid element was

conducted as shown in Figure 5.5. A pipe having the same diameter with a 50% circumferential through-wall crack was subjected to four-point bending. The moment–rotation curve is shown in Figure 5.6. The X-axis represents the additional rotation due to the crack, and it was calculated by subtracting the rotation of the uncracked pipe from the total crack of the cracked pipe. This curve was used as the connector element behavior.

A pipe with a through-wall crack undergoes crack opening, crack tearing, and, ultimately, complete pipe failure. Therefore, the moment-rotation curve has elastic, plastic, and damage moment regions, and these three parts are all considered in the study conducted by EMC^2 (Zhang et al., 2010). Actually, the load capacity of the cracked pipe should decrease during the crack tears; however, simulating these circumstances is very difficult. Therefore, only elasticity and plasticity were reflected in this thesis, with the assumption that the pipe can fail when the applied load reaches the limit load. As shown in Figure 5.6, the limit load of the 50% circumferential through-wall cracked pipe is 236 kN. For plasticity, an isotropic hardening rule was selected.

5.4 Decrease of applied load at crack position due to cr ack

Figure 5.8 and Figure 5.9 show the time history analysis results for the uncracked and cracked pipes. The load capacity at the crack position deceases by a large ratio in the crack pipe, and this can cause an increase in

the applied moment at the other part of the pipe. Generally, it is observed that the decrement increases with the applied load.

Figure 5.10 to Figure 5.12 summarize the moment decrement for each condition. The X- and Y-axes represent the applied moment at the crack position of the uncracked and the cracked pipe, respectively. Therefore, the closed the graph gets to y = x, the less is the behavior of the pipe affected by the crack.

5.4.1 Depending on pipe length

As mentioned in chapter 2, the seismic inertial moment due to the vibration belongs to the primary load. This means that M_{SI} continues without reference to how many plastic deformations occur. Therefore, it can be expected that a long pipe could be less affected by the crack than a shorter pipe. On the contrary, in a short pipe whose M_{SAM} is dominant, there could be a large difference between the uncracked and the cracked pipe in terms of the applied load.

Similarly, it is apparent from Figure 5.10 that the 5-m pipe has the largest ratio of load decrease. However, in the remaining cases, as the pipe length increases (proportion of M_{SI} increases), the load decrement increases although M_{SI} is the primary load, whereas a 20-m pipe has a large decrement of load. This indicates that if the primary and the secondary load are applied simultaneously, the loads could be applied differently than the general characteristics of loads.

5.4.2 Depending on crack position

A comparison of the results depending on the crack position shows that the load reduction ratio of the pipe with a crack near the anchor is greater than that of a pipe with a crack near the center. This is closely related to the applied load on the other part of the pipe. If a crack is located at position A, plastic deformation of the crack occurs first. However, if a crack is located at position B, the applied load on the other part is greater than at the crack position, and therefore, the normal pipe can deform before crack deformation. Then, the rotation at the crack can decreases. As a result, a pipe with a crack near the center could be less affected than one with a crack near the edge.

5.4.3 Depending on excitation mode

In terms of the excitation mode, there are large differences between the cases of 10- and 20-m pipes. However, it is difficult to observe a clear tendency between the two cases. The details about this will be dealt with in discussion.

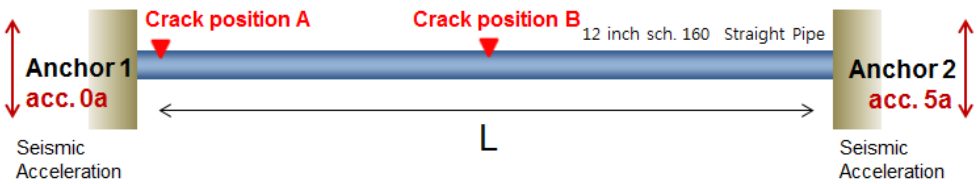

Figure 5.1 Modeling of cracked pipe

Table 5.1 Properties of cracked pipe

Pipe length	5m, 10m, 15m, 20m
Outer diameter	323.8 mm
Nominal thickness	33.3 mm
Number of nodes	101
Density	9.71 g/cm^3
Connector mass	295 g
Damping ratio	4%

Table 5.2 Acceleration scale factor: Crack position A

Applied load (Ratio to limit load of cracked pipe)	Acceleration scale factor			
	5 m	10 m	15 m	20 m
350%	20.09	53.79	28.02	9.51
300%	17.22	46.11	24.02	8.15
250%	14.35	38.42	20.02	6.79
190%	10.91	29.20	15.21	5.16
160%	-	-	-	-
130%	7.46	19.98	10.41	3.53
100%	-	-	-	-
70%	4.02	10.76	5.60	1.90
50%	-	-	-	-
20%	1.15	3.07	1.60	0.54

Table 5.3 Acceleration scale factor: Crack position B

Applied load (Ratio to limit load of cracked pipe)	Acceleration scale factor			
	5 m	10 m	15 m	20 m
350%	-	-	-	-
300%	-	159.94	66.26	14.78
250%	-	133.29	55.22	12.32
190%	-	101.30	41.96	9.36
160%	-	85.30	35.34	7.88
130%	-	69.31	28.71	6.41
100%	-	53.31	22.09	4.93
70%	-	37.32	15.46	3.45
50%	-	26.66	11.04	2.46
20%	-	10.66	4.42	0.99

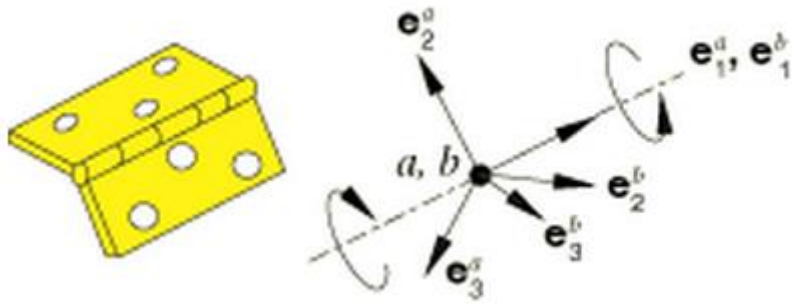

Figure 5.2 Connection type hinge(SIMULIA)

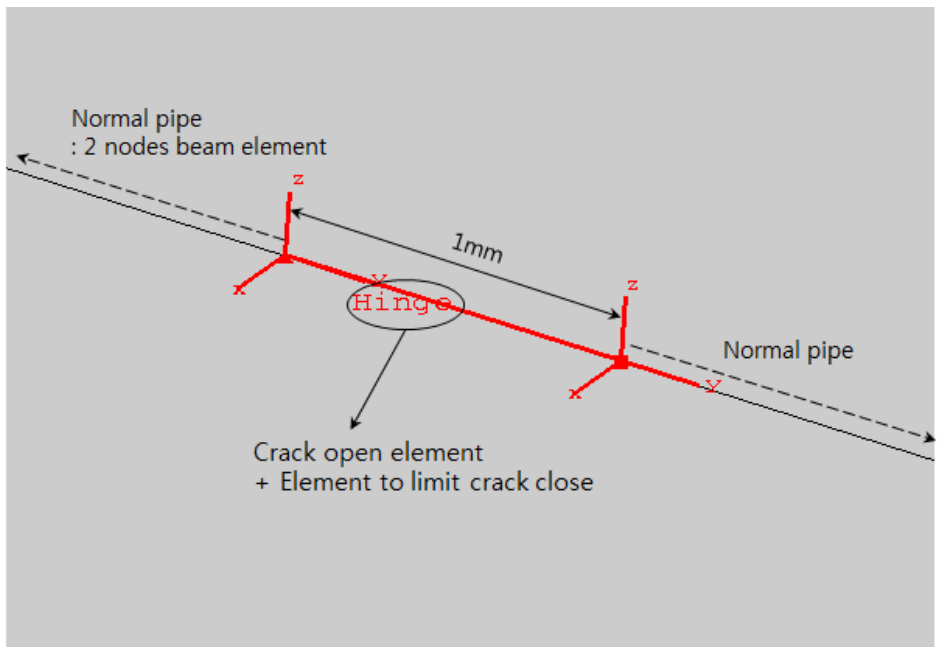

Figure 5.3 Arrangement of connector elements

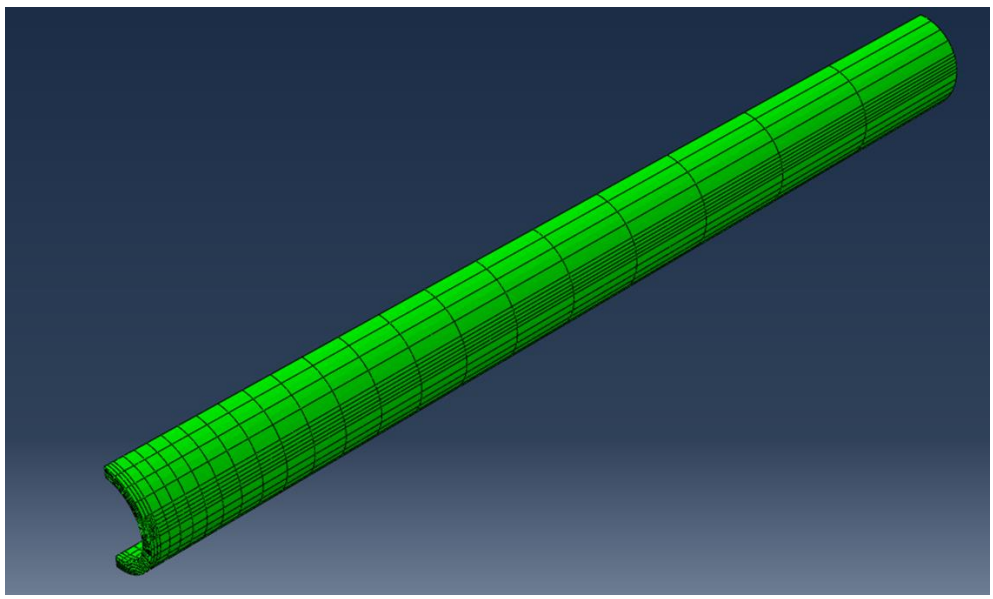

Figure 5.4 Modeling of through-wall cracked pipe using 3D solid element for finite element analysis

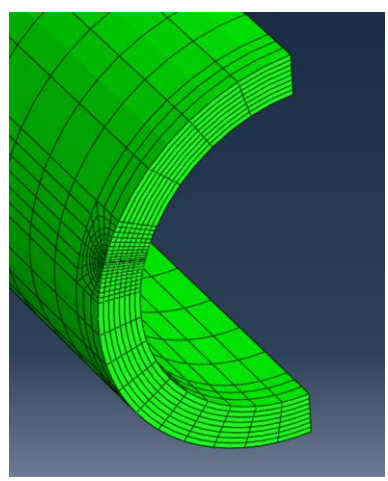

Figure 5.5 Details of mesh of crack

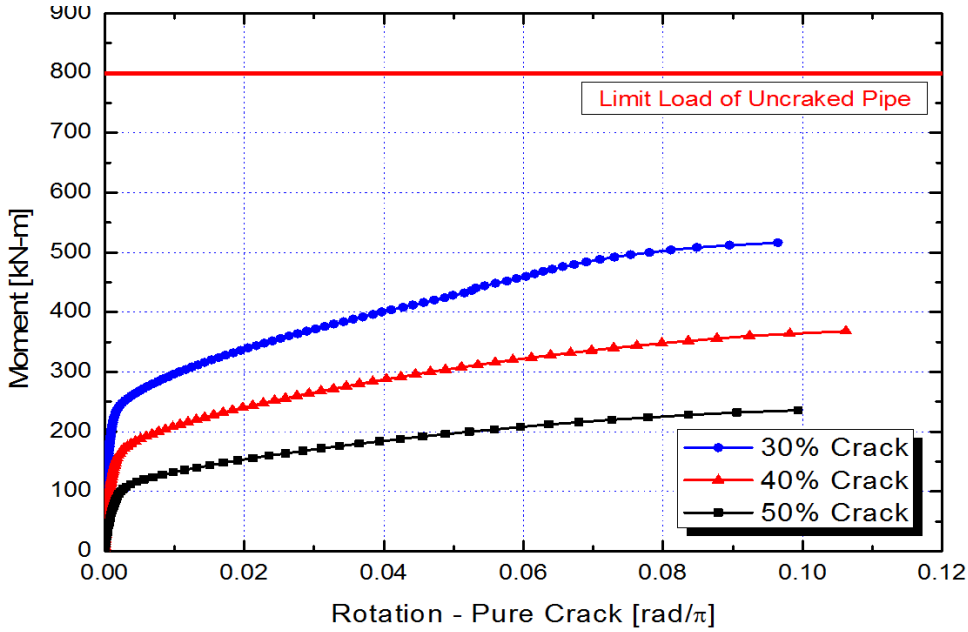

Figure 5.6 Moment-rotation curve of through-wall cracked pipe

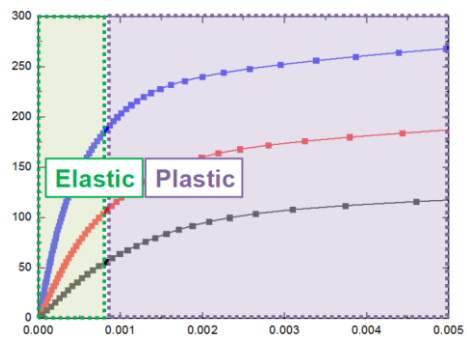

Figure 5.7 Separation to input connector element behavior

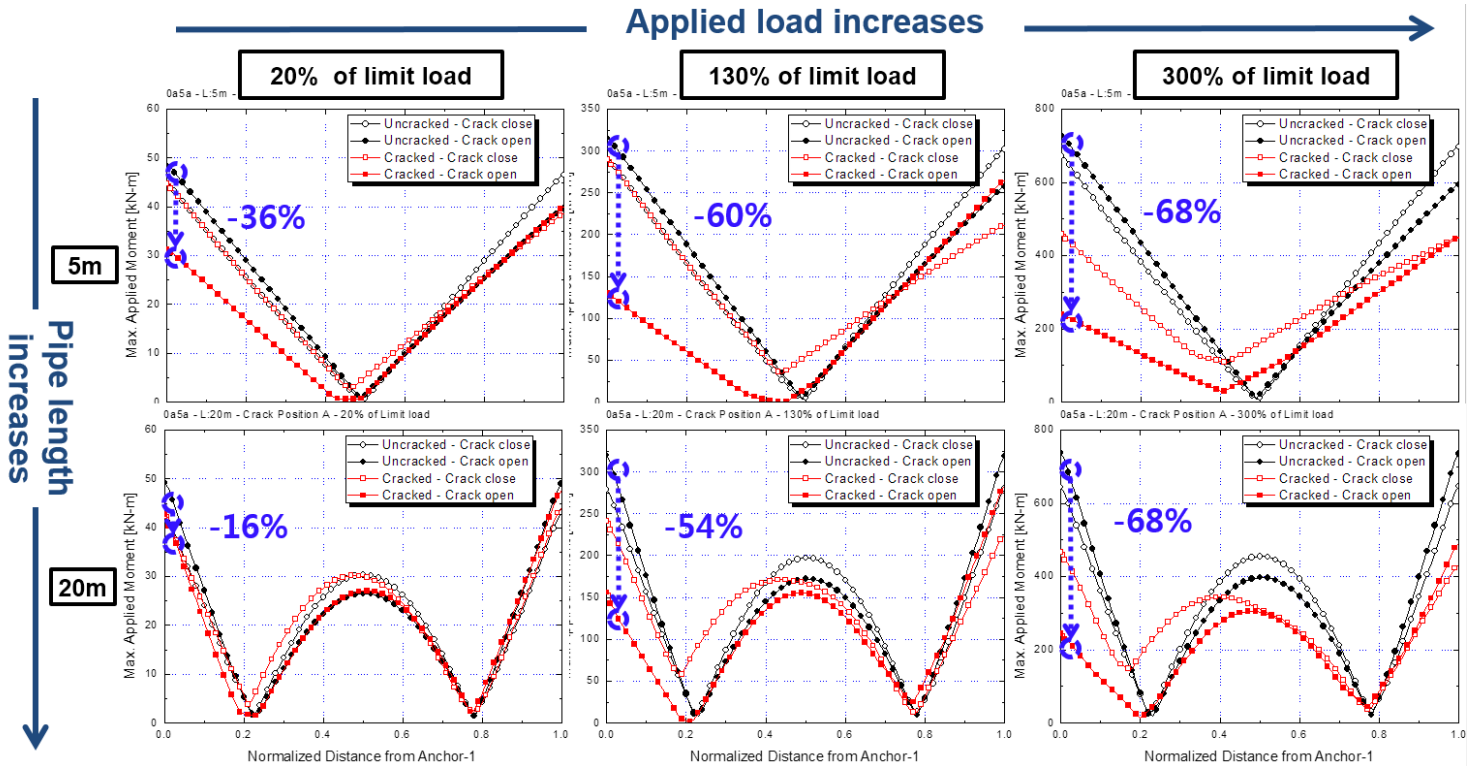

Figure 5.8 Result of cracked pipe analysis: Crack position A

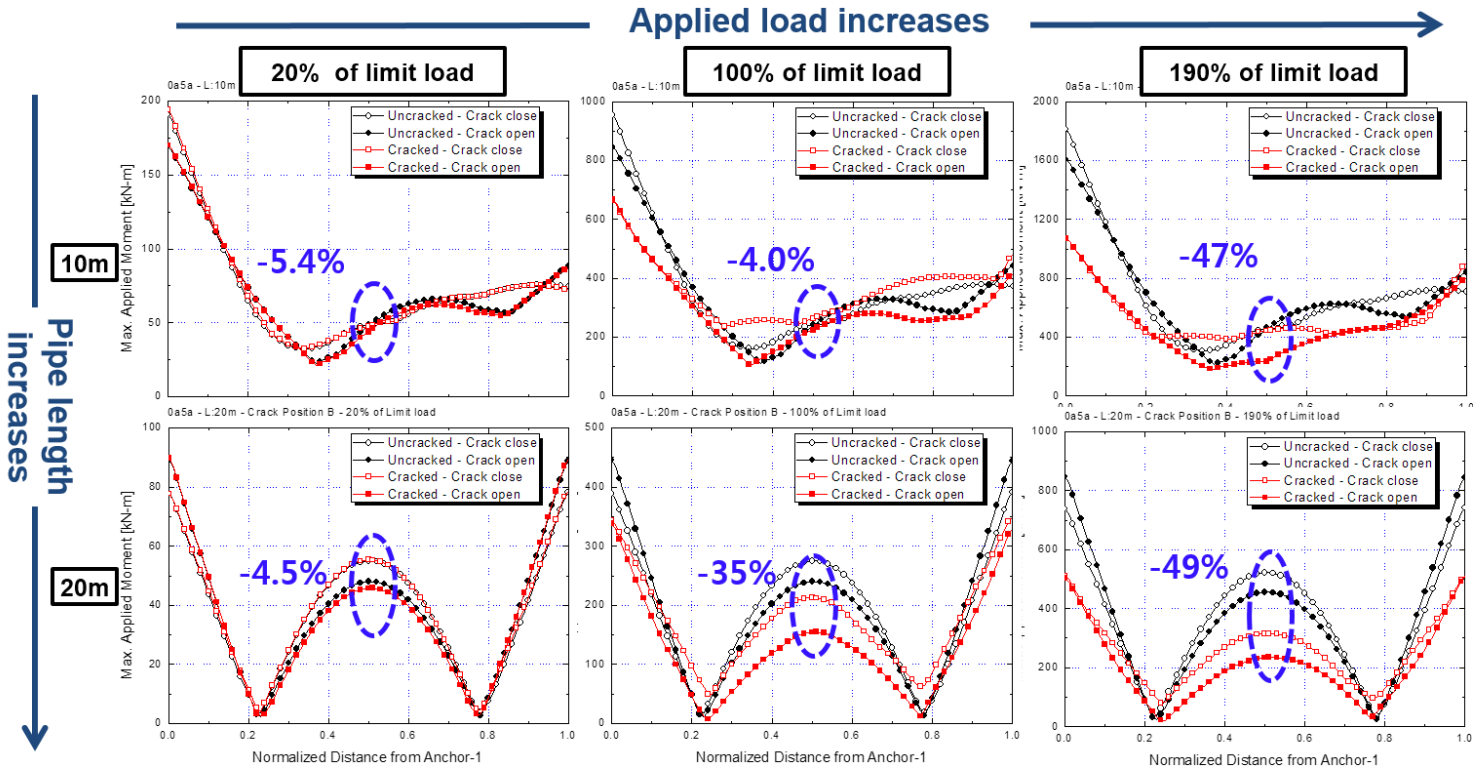

Figure 5.9 Result of cracked pipe analysis: Crack position B

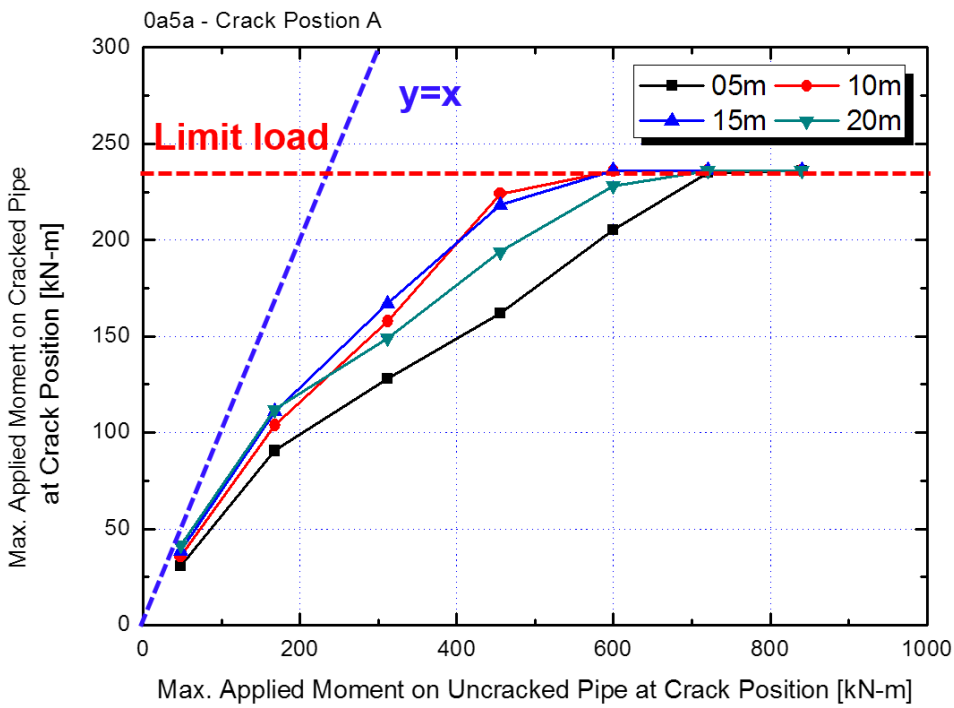

Figure 5.10 Tendency of decrease of applied moment at crack position : Crack position A, nonuiform excitation

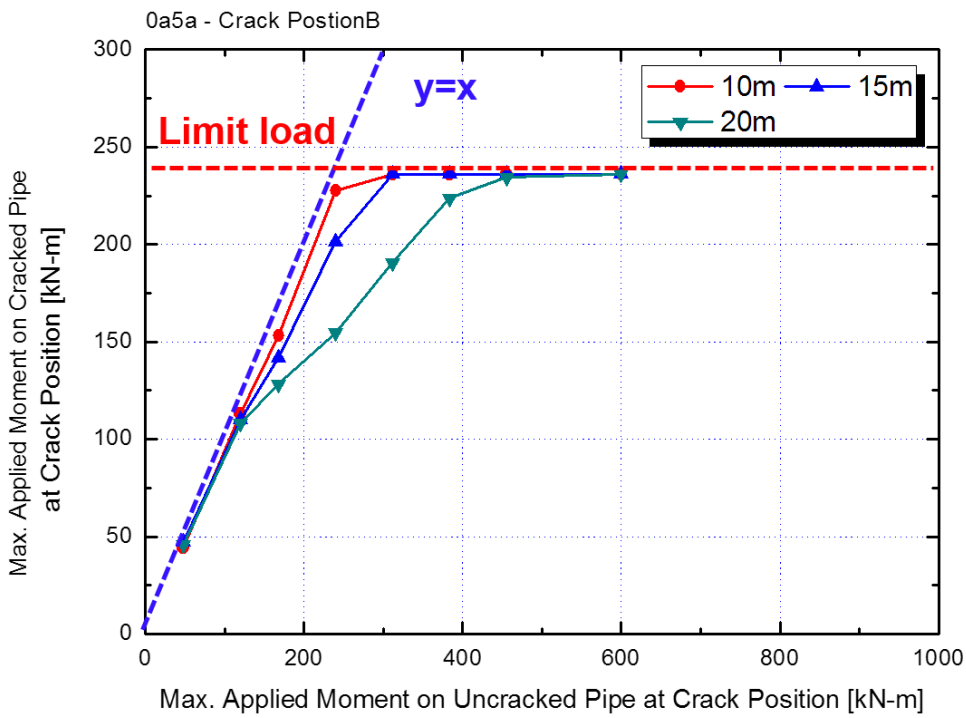

Figure 5.11 Tendency of decrease of applied moment at crack position : Crack position B, nonuniform excitation

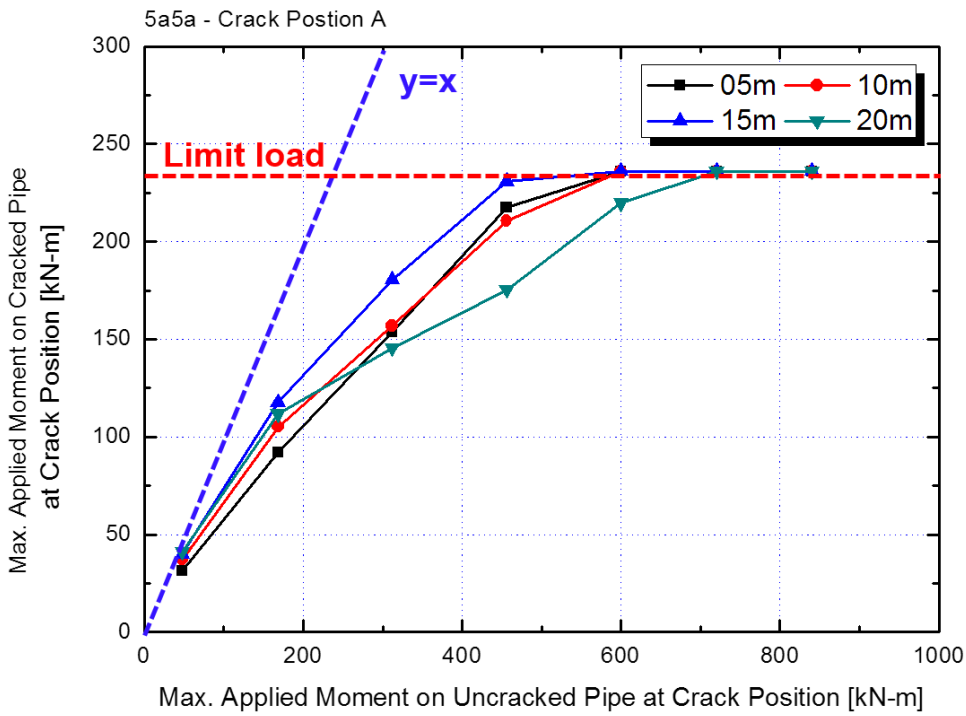

Figure 5.12 Tendency of decrease of applied moment at crack position : Crack position A, uniform excitation

Chapter 6 Discussion

6.1 Model simplification

The cracked pipe analysis results confirm that the applied load on the pipe can decrease by 4-70% owing to cracks; however, it is difficult to find a clear trend that can explain all cases. Therefore, additional calculations were performed using a simplified model and condition.

An elastic pipe was applied to exclude the effect of the plastic deformation of a normal pipe. The acceleration time history at the top of pipe region (5a) was used for both anchors to consider only the seismic inertial moment (M_{SI}). Finally, the analysis was conducted using only the pipe cracked at the edge (Position A).

Figure 6.1 shows the result of the additional analysis. It shows a clearer trend except for the 20-m pipe. The main questions are (i) the tendency depending on the pipe length except for the 20-m pipe and (ii) the reason why the 20-m pipe is exceptional

6.2 Static analysis

Static analysis was first conducted to understand the effect of a crack on

the entire piping system. Both anchors were fixed, and the distributed load was applied to the entire pipe.

Because seismic loading is a repeated load, the effect of hardening is very important. Therefore, a ramp load and sine wave load with three cycles were applied. Figure 6.3 and Figure 6.4 show the result of static analysis. As expected, the crack effect is largest when the pipe is short.

This can be understandable in terms of stiffness. The crack affected the stiffness of the pipe, the degree of which increased with a decrease in the pipe length. Therefore, the load capacity of the pipe decreased with its length. This result may explain the tendency depending on the pipe length except for the 20-m pipe.

In addition, considering that only M_{SI} was considered, if M_{SAM} is added on the pipe, the applied load can decrease by a larger proportion for a shorter pipe. This can explain the large difference between the 5-m pipe case and others in Figure 5.10.

6.3 Quasi static analysis

As the connection between static and dynamic analysis, a modified static analysis was conducted. The calculation method was basically the same as that in the static analysis, and a distributed load was applied. However, the load time history used as the input was derived from the dynamic analysis result. Using the compliance of each pipe length with the crack, the

equivalent distributed load can be obtained. The characteristics of the dynamic analysis caused by the damping ratio or natural frequency of the structure can partly be reflected in the analysis; we cannot consider this type of analysis method to be a perfect static analysis.

Figure 6.5 shows the result of quasi static analysis. The 20-m pipe still differs slightly from the trend; however, as noted in the previous paragraph, this could be because this analysis has the characteristics of the dynamic analysis. In comparison with Figure 6.1, there is a large difference from the result of the 20-m pipe. This indicates that the result of the 20-m pipe is related to the difference between the static and the dynamic analysis.

6.4 Time history of applied moment

Figure 6.6 and Figure 6.7 show the time history of the applied load for each pipe length; the black and red lines represent the results of the uncracked and the cracked pipes, respectively. A remarkable feature of this graph is the fact that the 20-m pipe case shows the largest phase difference.

Dynamic analysis is a procedure used to solve the equation of motion(Chopra, 1995), and therefore, the amplitude and phase of the response can be influenced by the natural frequency of the structure. Therefore, it is necessary to approach this problem in terms of the natural frequency.

6.5 Considering natural frequency

The natural frequencies of first and second mode vibrations are listed in Table 6.1, and Figure 6.8 shows the response spectra converted from the acceleration time history in the frequency domain.

The crack can reduce the stiffness of the pipe, leading to a decrease in the natural frequency. The reduction ratios of the natural frequency of each pipe are similar to each other within ~10%. However, as a result, the structure can experience vibrations of different intensities. For example, in the case of a 20-m pipe, the acceleration in accordance with the first mode frequency of the uncracked pipe is ~1.8g whereas that of the cracked pipe is ~1.5g, with the difference being ~0.3g. However, the difference for other pipes is less than 0.1g. This can explain why the 20-m pipe is exceptional.

As mentioned in section 5.4.3, this can be related to the difference between uniform and nonuniform excitations. Although it is difficult to determine the exact response spectra of the summation of two accelerations, there exists several conjectures in this regard. In the frequency range where the 1st mode frequency of the 20-m pipe exists, there exists a very rapid peak relative to the other peaks. Therefore, M_{SI} of the 20-m pipe is sensitive to the frequency distribution of the applied vibration. This explains why the result of the 20-m pipe differs greatly between the uniform and nonuniform excitation cases.

In summary, the effect of cracks on the pipe behavior is mainly affected by two factors. The first is the degree of influence of the crack on the stiffness of the entire structure. The second is the relation between the natural frequency of the structure and the frequency distribution of the applied vibration. If the applied load is sufficiently large so that pipe can deform in plastic way, the dynamic behavior of the pipe could become very complicated.

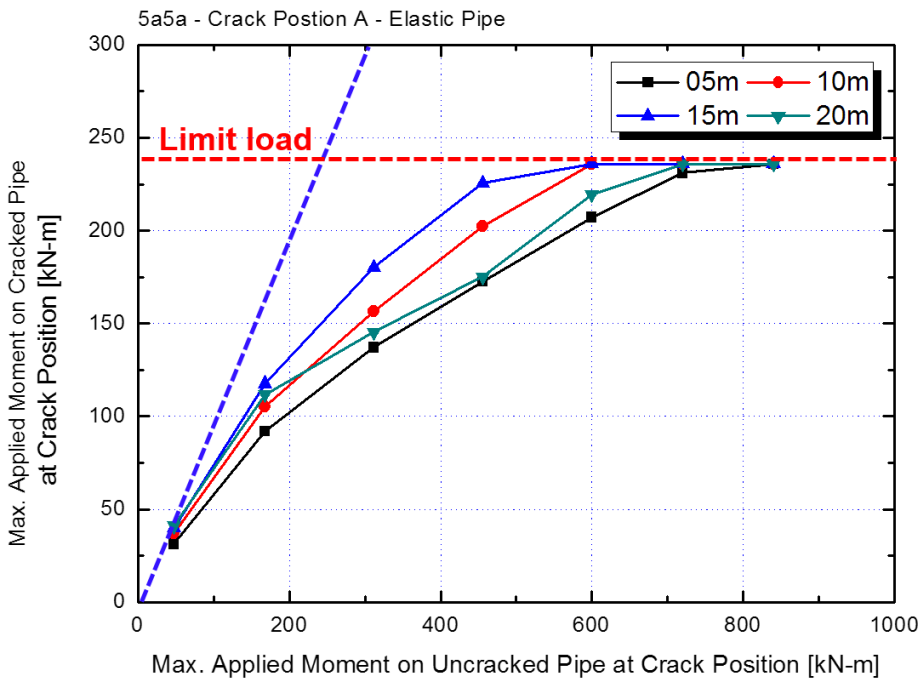

Figure 6.1 Tendency of decrease in applied moment at crack position : Crack position A, uniform excitation, elastic pipe

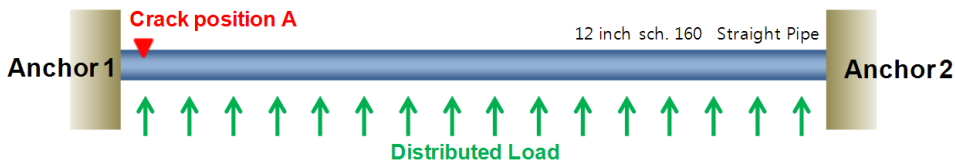

Figure 6.2 Modeling for static analysis

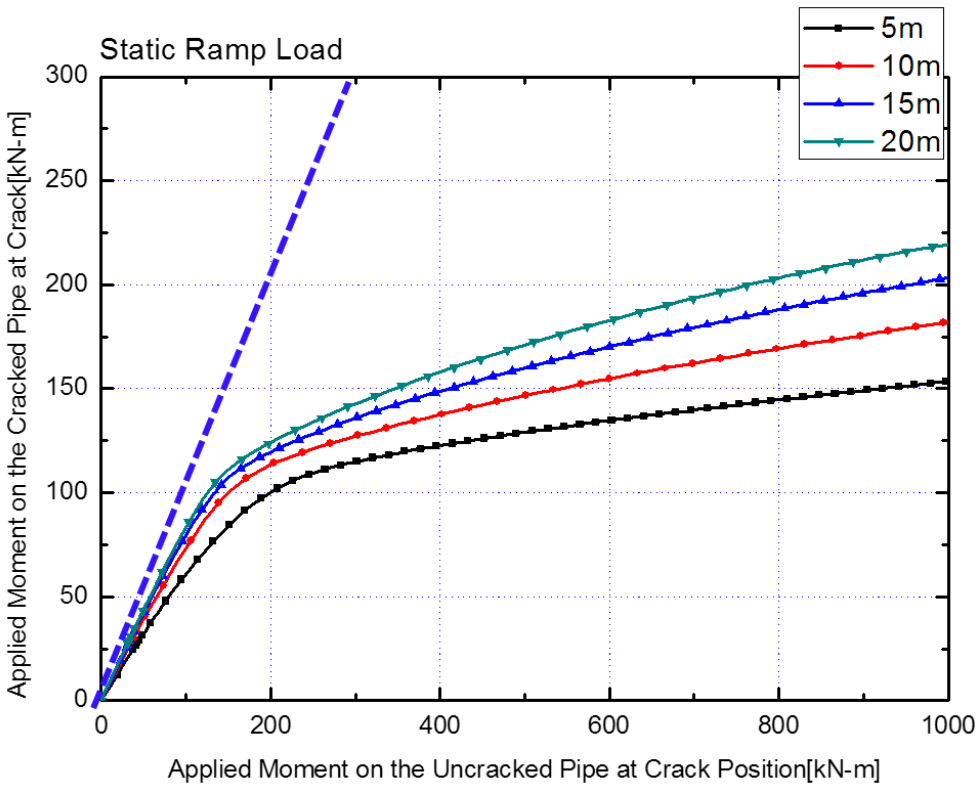

Figure 6.3 Tendency of decrease in applied moment at crack position : Crack position A, static ramp load, elastic pipe

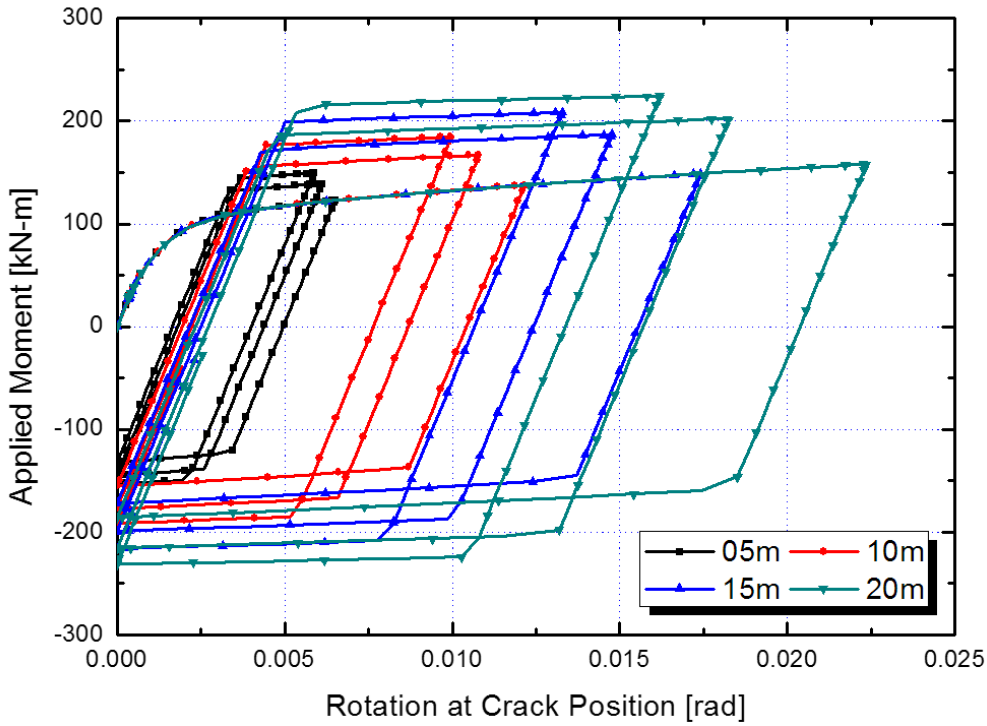

Figure 6.4 Moment history curve

: Crack position A, static cyclic load, elastic pipe

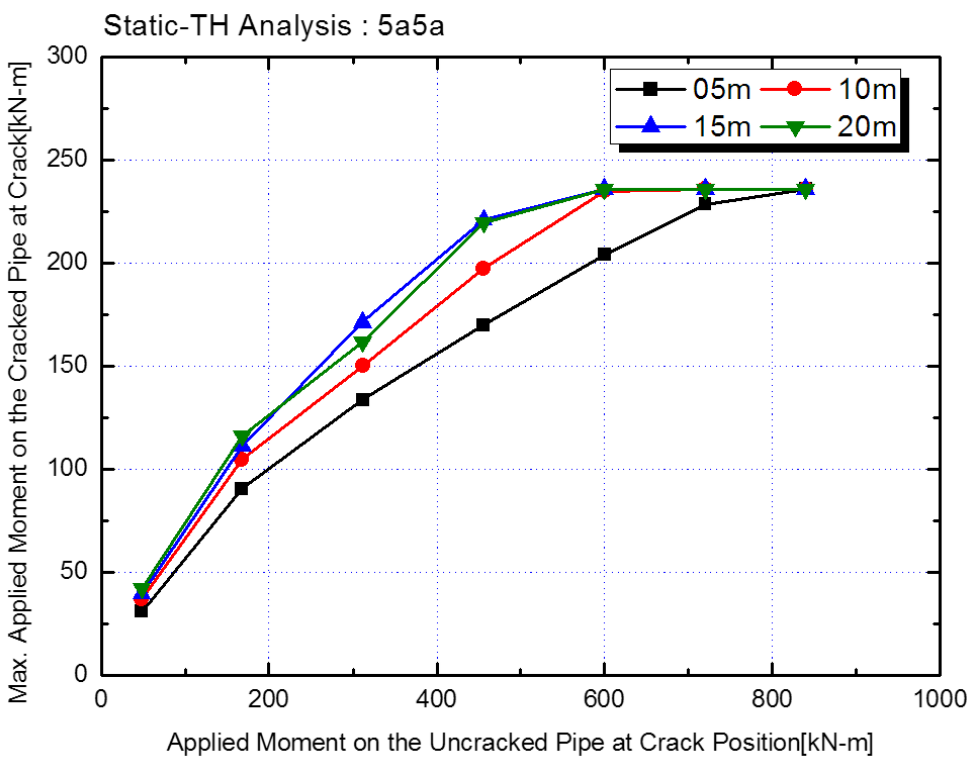

Figure 6.5 Tendency of decrease in applied moment at crack position : Crack position A, quasi static excitation, elastic pipe

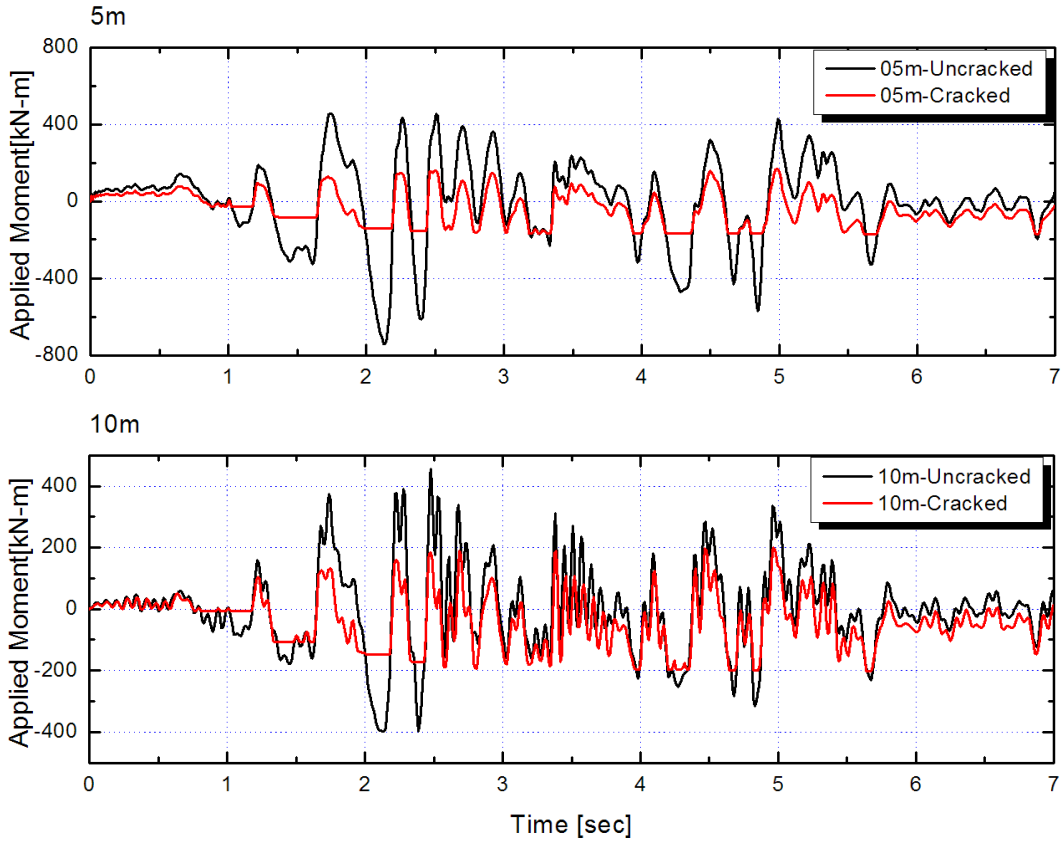

Figure 6.6 Time history of applied moment

: Crack position A, uniform excitation, elastic pipe

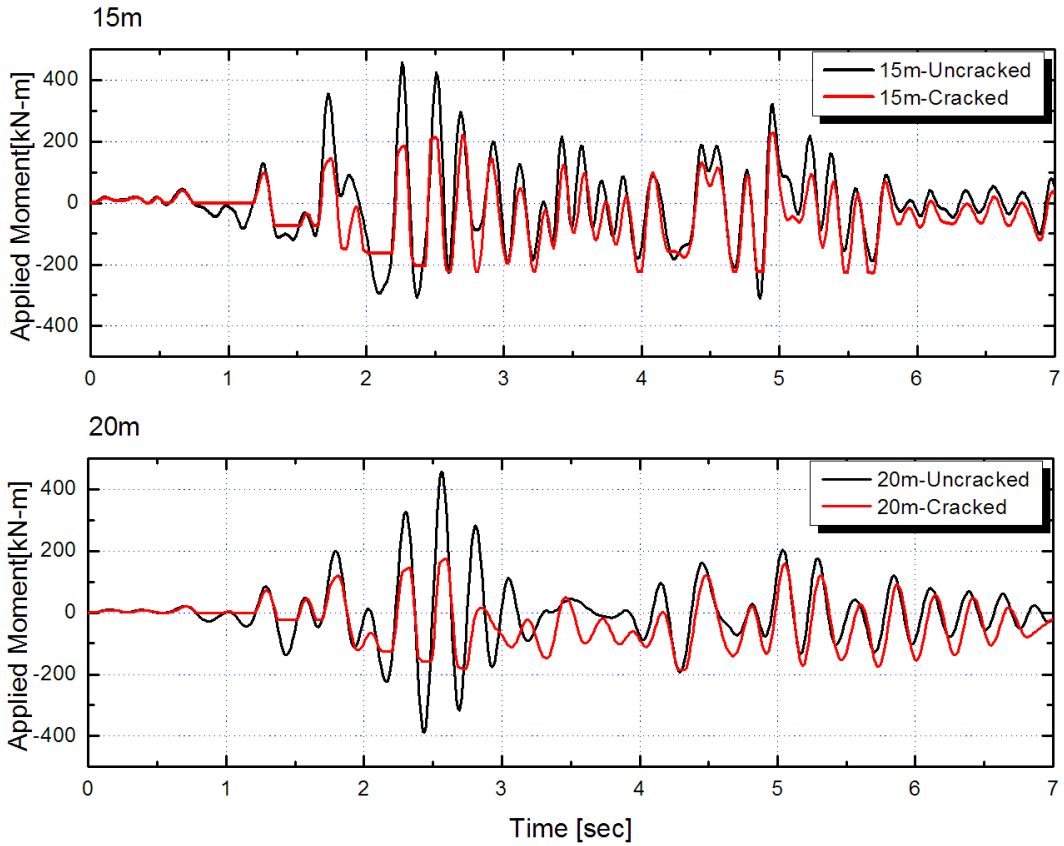

Figure 6.7 Time history of applied moment (continued)

: Crack position A, uniform excitation, elastic pipe

Table 6.1 Natural frequency of pipe

Natural Frequency [Hz]				
Pipe Length	**Uncracked**		**Cracked**	
	1st mode	**2nd mode**	**1st mode**	**2nd mode**
5m	58.91	153.41	51.328	140.45
10m	15.282	41.451	13.933	38.614
15m	6.8407	18.718	6.3884	17.702
20m	3.8577	10.589	3.6544	10.117

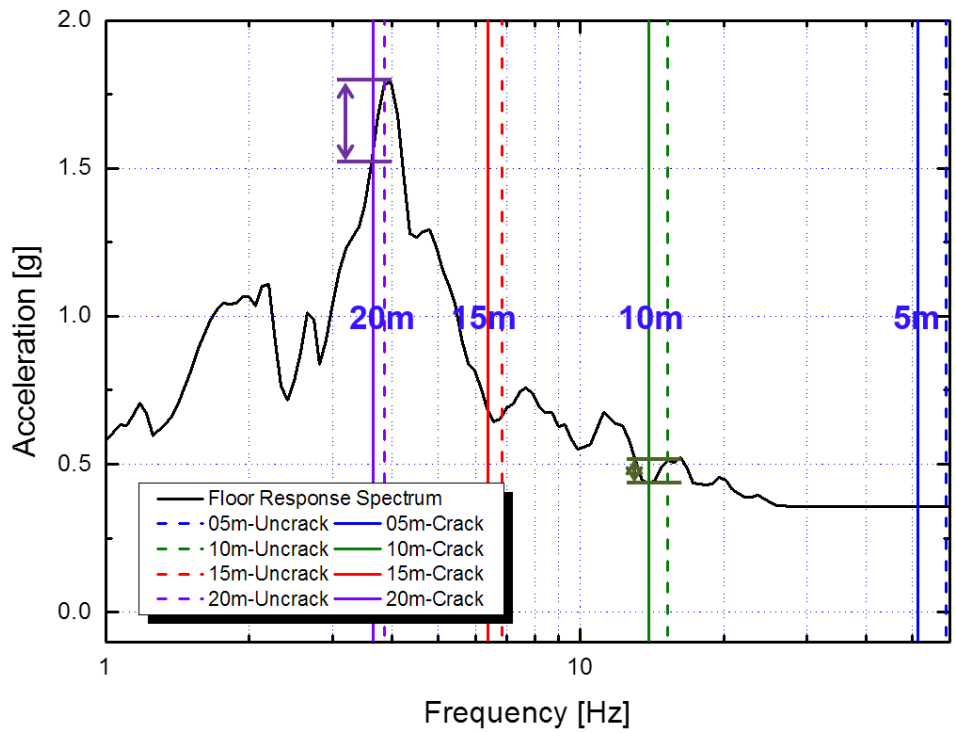

Figure 6.8 Response spectrum used in time history analysis, and natural frequency of each pipe length

Chapter 7 Conclusions and Future Work

7.1 Summary and findings

In this thesis, a seismic analysis of uncracked and cracked pipes was conducted to understand the dynamic behavior of the structure under a beyond design basis earthquake.

First, an uncracked pipe was analyzed using general seismic analysis and time history analysis. The distributions of the seismic inertial moment, which is calculated by response spectrum analysis, and the moment due to seismic anchor motion, which can be obtained from seismic anchor motion analysis, was confirmed depending on the pipe length. A comparison with the time history analysis result indicated that time history analysis generally provided a less conservative solution.

Various conditions were considered for cracked pipe analysis—pipe length, crack position, and the excitation mode. It was confirmed that the applied load on the pipe can decrease by 4-70% owing to cracks; however, it is difficult to find a clear trend that can explain all cases.

In additional, a calculation using a simplified model and conditions and a qualitative interpretation of the complicated cracked pipe analysis result were performed. The main factors that can affect the change in safety margin under seismic load are (i) the degree of the effect of a crack on the change in stiffness and (ii) the relation between the natural frequency of the structure and the applied vibration.

7.2 Future work

This study dealt with the loading induced by a beyond design basis earthquake. In the ASME B&PV Code, an operation service level D loading includes several types, one of which is seismic loading. Of course both static and dynamic loads are included, with their combination being of great importance. It is necessary to consider the interactions of various types of loads to obtain a more realistic solution. From this viewpoint, this study mainly aims to conduct an advanced analysis using a more realistic structural model and conditions.

The evaluation of the structural integrity of NPPs is changing from a deterministic approach to a probabilistic analysis. Specifically, in the piping system, it is essential to find a complete methodology to calculate the probability of pipe rupture and then reduce this probability. In addition to the applied load, many variables are considered in this process—material property, flaw inspection probability, crack behavior, etc(U.S. Nuclear Regulatory Commision, 2012c). To synthesize these variables, the exact prediction of the dynamic behavior of a pipe under particular conditions may be a key point. In addition, this can support a leak before break design. Therefore, the ultimate application of this thesis result is defined to provide complete measures for probabilistic fracture mechanics.

Bibliography

ASME. Boiler and pressure Vessel Code *Section XI : Rules for Inserv ice Inspection of Nuclear Poser Plant Components*.

ASME. Boiler and pressure Vessel Code *Section III : Rules for Const ruction of Nuclear facility Components*.

Chopra, A. K. (1995). *Dynamics of structures: theory and applications to earthquake engineering* (Vol. 2). Upper Saddle River, NJ: P rentice Hall.

El Centro Earthquake Vibrationdata. *http://www.vibrationdata.com/elcent ro.htm*.

F. Godefroy. (2012). Pre-Construction Safety Report *Chapter 15: Prob abilistic safety analysis* AREVA NP.

Gorman, J., Hunt, S., Riccardella, P., & White, G. A. (2009). PWR R eactor Vessel Alloy 600 Issues: ASME.

Ian, H.-l. Nuclear Power Plants and Earthquakes *Encyclopedia of Eart h Topics*: World Nuclear Asscociation.

KINS. (2013). Guidelines for Nuclear Power Plant Stress Test (in Kor ean).

Korea Hydro & Nuclear Power Company. (2013). Final Report : Repo rt of Stress tess for Wolsung 1 (in Korean).

Nam, I. k., Bae, J. h., Huh, S. h., & Kim, S. k. (2011). Technical R eview on Application of New Seismic Rules to Piping Design: KOPEC E&C.

Reed, J., Kennedy, R., Buttemer, D., Idriss, I., Moore, D., Barr, T., . . . Smith, J. (1991). A methodology for assessment of nuclear power plant seismic margin: Electric Power Research Institute, NP-6041.

Selby, G., & Harrington, C. (2009). Materials Reliability Program: Development of Probability of Detection Curves for Ultrasonic Examination of Dissimilar Metal Welds: Electric Power Research Institute.

Seo, Y.-D. (2013). *An Experimental Study of the Nuclear Power Plant Piping System under Ultimate Loading Conditions*. (Master), Pusan National University.

SIMULIA. *Abaqus 6.12 documentation : Abaqus Analysis User's Manual*.

Suzuki, K., & Kawauchi, H. (2008). *Test Programs for Degraded Core Shroud and PLR System Piping: Seismic Test Results and Discussion on JSME Rules Application.* Paper presented at the ASME Pressure Vessels & Piping conference.

Suzuki, K., Kawauchi, H., & Abe, H. (2006). *Test Programs for Degraded Core Shroud and PLR Piping: Simulated Crack Models and Input Seismic Waves for Shaking Test.* Paper presented at the ASME Pressure Vessels & Piping conference.

U.S. Nuclear Regulatory Commision. (1978). Regulatory Guide 1.122: Development of Floor Design Response Spectra for Seismic Design of Floor-Supported Equipment or Components, (Revision 1).

U.S. Nuclear Regulatory Commision. (2007a). *Regulatory Guide 1.61: Damping values for seismic design of nuclear power plants, (Revision 1).*

U.S. Nuclear Regulatory Commision. (2007b). Regulatory Guide 1.208 : A performance-based approach to define the site-specific eart hquake groundmotion.

U.S. Nuclear Regulatory Commision. (2007c). Standard Review Plan 3. 7.1 : Seismic Design Parameters, (Revision 3), NUREG-0800.

U.S. Nuclear Regulatory Commision. (2009). Interim Staff Guidance o n implement of a Probabilistic Risc Assessment-Based Seismic Margin Analysis for New Reactors, DC/COL-ISG-020.

U.S. Nuclear Regulatory Commision. (2012a). Guidance on Performing a Seismic Margin Assessment in Response to the March 2012 Request for Information Letter, ML12222A327.

U.S. Nuclear Regulatory Commision. (2012b). Regulatory Guide 1.92 : Combining Modal Responses and Spatial Components in Sei smic Response Analysis, (Revision 3).

U.S. Nuclear Regulatory Commision. (2012c). xLPR Pilot Study Repor t, NUREG-2110.

Wilkowski, G., Brust, B., Zhang, T., Hattery, G., Kalyanam, S., Shim, D.-J., Johnson, J. (2011). *Robust LBB Analyses for Atucha II N uclear Plant*. Paper presented at the ASME Pressure Vessels & Piping conference.

Yoon, J. Y., Kim, Y. J., Hwang, I. S., Ayers, L., Short, M., Bromberg, L., & Ballinger, R. G. (2013). *On-line Monitoring of Artificial crack in Piping Weldment Using Array Probed Direct Current Potential Drop*. Paper presented at the ASME Pressure Vessels & Piping Conference.

Zhang, T., Brust, F. W., Shim, D., Wilkowski, G., Nie, J., & Hofmaye r, C. (2010). Analysis of JNES Seismic Tests on Degraded Pipi ng, NUREG/CR-7015.

Zhang, T., Brust, F. W., Wilkowski, G., Xu, H., Betervide, A. A., & Mazzantini, O. (2012). *Beyond Design Basis Seismic Analysis for Atucha II Nuclear Plant.* Paper presented at the 2012 20th International Conference on Nuclear Engineering and the ASME 2012 Power Conference.

Zhang, T., Brust, F. W., Wilkowski, G., Xu, H., Betervide, A. A., & Mazzantini, O. (2013). Leak-Before-Break Under Beyond Design Basis Seismic Loading. *Journal of Pressure Vessel Technology, 135*(5), 051801.

초 록

원자력발전소의 설계와 건설기술이 발전하면서 신규 발전소에 적용되는 안전정지지진(SSE) 규모가 증가하고 있다. 그러나 후쿠시마 사고를 비롯하여 설계기준을 초과하는 사건의 발생이 잦아짐에 따라 후속조치의 일환으로 유럽 및 국내에서는 최근 노후 원전에 대해 스트레스 테스트를 수행하고 있다. 이 과정에서는 발생 가능한 지진의 규모에 대해 확률론적으로 접근하여, 원자력발전소가 설계기준보다 큰 규모의 지진에 대해서도 안전정지 성능과 건전성을 유지할 수 있는지에 대한 평가가 수행된다. 이러한 관점에서, 배관에 대해서도 설계기준을 넘어서는 지진에 대한 내진 성능 평가가 이루어져야 한다.

또한 노후화된 원전에 대해서 수명연장이 추진됨에 따라 구조물의 건전성을 감시, 관리하는 것이 중요해졌으며, 가압경수로 1차측 배관 용접부의 경우 다양한 환경영향 요인에 의해 균열이 발생할 확률이 높기 때문에 특히 주의를 요한다. 따라서 구조물의 균열을 검출하기 위한 비파괴 검사법이 10년 주기마다 수행되고 있으며, ASME B&PV Code Sec. XI 에서는 다음 주기까지의 운전여부를 판단하기 위한 허용 결함 크기를 제시하고 있다. 그럼에도 불구하고 허용크기를 넘어서는 균열이 발견된 사례들은 배관의 내진 해석 있어 균열에 대한 고려가 필수적임을 시사한다. 이에 본 연구는 지진하중 하에서 비균열 배관과 균열 배관의 동적 거동에 대한 분석을 수행하고자 하였다.

ASME B&PV Code Sec. III에 따르면 지진에 의해 구조물이 받게 되는 하중은 진동에 의한 관성 하중(M_{SI})과 앵커의 상대변위로 인해 발생하는 앵커운동하중(M_{SAM})으로 구분할 수 있다. 응답스펙트럼 해석을 통해 관성 하중을 구할 수 있고, 앵커운동해석을 통해 앵커운동하중을 도출할 수 있으며 이는 일반 설계절차에 포함된다. 이 접근을 통해서는 두 하중을 따로 구하게 되지만 시간이력해석 방법은 두 하중을 동시에 고려할 수 있으며 더 현실적인 해를 얻을 수 있어 동적 거동의 분석에 적합하다. 본 연구에서는 유한요소해석프로그램인 ABAQUS를 사용하여 각 해석방법의 이해를 도모하고, 시간이력 해석법을 비균열 배관 및 원주방향 관통균열 배관에 대해 수행하여 그 동적 거동을 비교하는 것을 목적으로 하였다.

먼저 비균열 배관에 대해 일반 설계절차를 따른 해석이 수행되었고 배관의 길이에 따른 관성하중과 앵커운동하중의 기여도를 평가하였다. 또한 시간이력해석을 추가로 해석한 뒤 그 결과를 일반설계해석과 비교하여 일반 설계절차가 더 보수적인 결과를 도출함을 확인하였다.

또한 ABAQUS의 연결요소 중 하나인 힌지(Hinge)를 사용하여 균열을 표현한 배관에 대해서 다양한 상황 하에 시간이력해석을 수행하였다. 비균열 배관의 해석결과와 비교하여 배관길이, 균열 위치, 인가 하중의 형태나 크기에 따라 균열부에 작용하는 하중은 4~70% 비율로 감소함을 확인하였으나 모든 상황에 대한 일관적인 경향성을 찾기에는 결과가 복잡했다. 따라서 앞선 결과를 설명할 수 있는 근거를 찾기 위해 단순화된 모델을 사용한 추가해석을 수행하였다. 그 결과 배관의 동적 거동에 큰 영향을 줄 수 있는 인자는 크게 (1) 균열이

배관의 강성에 미치는 영향과, (2) 구조물의 고유진동수와 구조물에 인가된 진동의 진동수 분포와의 관계임을 확인하였다.

최근 원자력발전소 구조물의 건전성 평가는 결정론적인 방법에서 확률론적인 방법으로 그 접근법이 변화하고 있다. 다양한 상황에 대해서 배관의 동적 거동을 이해하는 것은 배관의 파단확률을 계산하는 데 큰 도움이 될 수 있다. 이를 위해서 본 연구는 여러 배관의 형상에 대한 이해를 도모하고, 지진하중뿐만 아니라 정상운전하중을 포함한 다양한 하중을 함께 고려함으로써 개선되어야 할 것이며, 그럼으로써 확률론적 파괴역학에 있어 효율적인 도구가 될 수 있을 것이다.

주요어 : 배관 내진 해석, 설계기준 초과 지진, 시간이력해석법, 원주방향 관통균열 배관, 지진 관성 하중, 앵커 운동 하중

학 번 : 2012-20994

감사의 글

작은 결실과 함께 석사과정 2년의 시간을 마무리하며, 감사했던 분들께 짧게나마 인사를 전하려 합니다.

아무것도 몰랐던 학부 1학년 때부터 면담을 해오면서 교수님께 지도를 받겠다고 다짐했던 기억이 납니다. 그 때의 다짐이 이어져 지금까지 오게 되었습니다. 앞길 보는 데만 급급했던 저의 시야를 넓혀 주시고 도전적인 과제를 안겨주신 황일순 교수님, 정말 감사 드리고 앞으로도 큰 가르침 받을 수 있도록 노력하겠습니다.

연구의 자세조차 몰랐던 저를 이끌어 주시느라 많이 갑갑하셨을 텐데 차분히 가르쳐 주신 오영진 박사님, 몇 달 동안 정말 많은 것을 배웠습니다. 감사 드립니다. 그리고 Oda 교수님, 한국에서 첫 논문지도 제자가 된 것을 영광스럽게 생각합니다. 최영환 박사님, 김윤재 교수님, 김종성 교수님, 바쁘신 와중에도 저의 부족한 질문에 친절하게 답변해주셔서 많은 도움이 되었습니다.

지난 2년을 곱씹어 보면 연구실에 공헌한 것은 없지만 연구실 식구들께 참 많이 의지해왔다고 느낍니다. 대선배로서 많은 도움 주시고 격려해주신 태현오빠, 경하오빠, 효온오빠, 묵묵히 할 일을 다하며 모범이 되셨던 승기오빠, 고민을 잘 털어놓지 못하는 저를 이야기하도록 이끌어 준 성열오빠, 분위기를 휘어잡던 성민오빠, 볼 때마다 발랄하게 인사해주는 지훈오빠, 학교 안에서도, 밖에서도 제 수많은 물음에 친절하게 알려준 효숙언니, 센스있는 일처리의 달인 재현오빠, 항상 저를 예뻐해주고 힘을 실어 주었던 영아언니, 지금은 함께 있지 않지만

감사했던 기억 안고 있습니다. 본인도 많은 고민 하면서 아낌없이 조언해 주셨던 원창오빠, 때론 짖궂어도 진지하게 충고해 주시는 현엽오빠, 저 때문에 많이 시달렸을 윤재영오빠, 실없는 말장난에 반응을 잘 해주는 박재영오빠, 왠지 친오빠처럼 대하고 싶은 정윤오빠, 입담도 일처리도 시원시원한 용훈오빠, 인생 선배로서 말씀 많이 해주신 영광오빠 모두 감사합니다. 성준이 희재, 산해에게는 특히 연구실 동료이자 동기라서 투정을 유난히 많이 부렸는데 다 받아주느라 정말 고생 많았고 앞으로도 잘 부탁할게.

대학원 오면서 자주 연락하지는 못했지만 08학번 동기들 앞으로 지내면서 서로 의지하면 참 좋을 것 같아. 특히 민화 혜정아, 마음을 여는 데 오랜 시간이 걸렸는데도 살갑게 대해줘서 고마워. 그리고 힘들다고 하소연 할 때마다 곁에서 묵묵히 들어주고 격려해 주었던 일웅, 너무 기대기만 한 것 같아 항상 미안하고 고맙고, 계속 행복한 추억 많이 만들어 나갔으면 해.

맨날 잔소리에 듣기 싫은 소리만 해도 그래도 누나라고 항상 잘 따라준 현섭. 표현은 잘 못해도 마음 알 거라고 믿고 앞으로도 우리 특별한 남매 사이를 잘 유지하자. 그리고 마지막으로 바쁘다는 핑계로 투정 부리고 맏딸 노릇 제대로 못하면서 철없게 굴어도 항상 응원해 주시고 밤낮으로 제 생각 해주신 우리 부모님 사랑합니다. 부모님의 은혜에는 한참 모자라겠지만 이 논문이 부모님의 희생에 조금이나마 보답이 되었으면 합니다.

2014년 1월

김예지 드림